University of Kentucky
UKnowledge

Theses and Dissertations--Medical Sciences | Medical Sciences

2019

RAPID NO• MEASURES IN RAT NUCLEUS ACCUMBENS AND FRONTAL CORTEX FOLLOWING NASAL ADMINISTRATION OF NITROGLYCERIN

Victoria A. Scott
University of Kentucky, victoria.a.scott@uky.edu
Digital Object Identifier: https://doi.org/10.13023/etd.2019.235

Right click to open a feedback form in a new tab to let us know how this document benefits you.

Recommended Citation

Scott, Victoria A., "RAPID NO• MEASURES IN RAT NUCLEUS ACCUMBENS AND FRONTAL CORTEX FOLLOWING NASAL ADMINISTRATION OF NITROGLYCERIN" (2019). *Theses and Dissertations--Medical Sciences*. 11.
https://uknowledge.uky.edu/medsci_etds/11

This Master's Thesis is brought to you for free and open access by the Medical Sciences at UKnowledge. It has been accepted for inclusion in Theses and Dissertations--Medical Sciences by an authorized administrator of UKnowledge. For more information, please contact UKnowledge@lsv.uky.edu.

STUDENT AGREEMENT:

I represent that my thesis or dissertation and abstract are my original work. Proper attribution has been given to all outside sources. I understand that I am solely responsible for obtaining any needed copyright permissions. I have obtained needed written permission statement(s) from the owner(s) of each third-party copyrighted matter to be included in my work, allowing electronic distribution (if such use is not permitted by the fair use doctrine) which will be submitted to UKnowledge as Additional File.

I hereby grant to The University of Kentucky and its agents the irrevocable, non-exclusive, and royalty-free license to archive and make accessible my work in whole or in part in all forms of media, now or hereafter known. I agree that the document mentioned above may be made available immediately for worldwide access unless an embargo applies.

I retain all other ownership rights to the copyright of my work. I also retain the right to use in future works (such as articles or books) all or part of my work. I understand that I am free to register the copyright to my work.

REVIEW, APPROVAL AND ACCEPTANCE

The document mentioned above has been reviewed and accepted by the student's advisor, on behalf of the advisory committee, and by the Director of Graduate Studies (DGS), on behalf of the program; we verify that this is the final, approved version of the student's thesis including all changes required by the advisory committee. The undersigned agree to abide by the statements above.

Victoria A. Scott, Student

Dr. Greg A. Gerhardt, Major Professor

Dr. Melinda Wilson, Director of Graduate Studies

RAPID NO• MEASURES IN RAT NUCLEUS ACCUMBENS AND FRONTAL CORTEX FOLLOWING NASAL ADMINISTRATION OF NITROGLYCERIN

THESIS

A thesis submitted in partial fulfillment of the requirements for the Master of Science in

the College of Medicine at the University of Kentucky

By

Victoria A. Scott

Lexington, Kentucky

Director: Dr. Greg A. Gerhardt, Professor of Neuroscience

Lexington, Kentucky

February 21, 2019

Copyright Victoria A. Scott 2019

ABSTRACT OF THESIS

RAPID NO• MEASURES IN RAT NUCLEUS ACCUMBENS AND FRONTAL CORTEX FOLLOWING NASAL ADMINISTRATION OF NITROGLYCERIN

Nitric Oxide (NO) is a powerful endogenous free radical that has numerous biological functions including vasodilation and serves as a post synaptic second messenger in the central nervous system (CNS). Numerous studies implicate NO• involvement in CNS disorders such as schizophrenia and drug abuse. These studies address the direct *in vivo* determination of an FDA-approved NO• donor (nitroglycerin) on extracellular levels of NO• in the frontal cortex and core of the nucleus accumbens in a lightly anesthetized rat. State-of-the-art *in vivo* amperometric recording techniques coupled with a novel 4-channel low noise pre-amplifier system and new generation microelectrode arrays (MEAs) will be used to record extracellular levels of NO• at 100Hz before and during nasal administration of either placebo (1) or nitroglycerin. This studies will determine the feasibility of measuring NO• in the CNS while administering the NO• donor nasally and determine the amplitude and kinetic time course effects of a nasally delivered NO• donor in two rat brain areas, the frontal cortex and core of the nucleus accumbens.

KEYWORDS: Nitric Oxide, Nucleus Accumbens, Frontal Cortex

Victoria A. Scott

February 21, 2019

RAPID NO• MEASURES IN RAT NUCLEUS ACCUMBENS AND FRONTAL CORTEX FOLLOWING NASAL ADMINISTRATION OF NITROGLYCERIN

By

Victoria Scott

Greg A. Gerhardt
Director of Thesis

Melinda Wilson
Director of Graduate Studies

February 21, 2019

Dedicated to Wayne and Karen Scott

My only hope is that with every passing day and degree I become even the slightest bit more like the two of you. Thank you for your love, support and readiness to always celebrate my life accomplishments with champagne.

Acknowledgments

I have attended three universities at the time this thesis was written and defended. While I have enjoyed my research ventures at each institution, my time at the University of Kentucky will remain uniquely challenging and transformative. The support, trust and push to peruse my own questions and — yes — often find my own answers has shaped me into a more confident and capable individual. I would like to acknowledge the role that the University of Kentucky College of Medicine played in my ability to conduct high level graduate research in a short period of time without barrier or condition. The embracement of research is what makes UK stand out as an exceptional Kentucky educational institution. I would like to acknowledge professors Wilson, Vander Kooi, Grondin and Franklin for their direction throughout the coursework of my masters. In particular, I would like to thank Drs. Grondin and Franklin for their continued support and flexibility throughout the course of my thesis preparation and defense. Although the day for defense of my thesis sometimes felt as though it would never come, you both helped make it possible.

I would like to acknowledge the Gerhardt lab and the support and direction of Dr. Gerhardt, Francois Pomerleau and Peter Huettl. I estimate I asked each of you over a thousand questions through the course of my benchwork and you responded with patience, understanding and tolerance. Furthermore, when parts of my experimentation went wrong, as is customary in research, you helped pick up my spirit and directed me forward to plan B. I thank you for all of the moral and educational support you provided over the past year.

Table of Contents

Acknowledgments iii

Table of Contents iv

List of Tables viii

List of Figures ix

Chapter One: Introduction and Outline 1

Nitric oxide 1

Synthesis and signaling 2

Decay and removal 3

Nitroglycerin 4

Frontal Cortex 5

Nucleus Accumbens 6

Intranasal Drug Administration 6

Thesis Outline 9

Chapter Two: MEA Electrochemistry, Fabrication and Calibration 15

MEA Fabrication 15

Solutions Used 15

diethylenetriamine (DETA)/ nitric oxide adduct 15

5 mM m-Phenylenediamine 15

mPD Coating 16

Ag/AgCl Reference Coating 16

Calibration 17

Chapter Three: Materials and Methods 26

Animals 26

Experimental Design 26

Randomization and Blinding 27

Test and Control Articles 27

Nasal Administration 28

Controls 28

Husbandry and Veterinary care 28

Animal Housing 28

Dietary materials 28

Procedures 29

Surgical Procedure 29

Experimental Procedure 32

Euthanization 35

Adverse Outcomes 35

Record Retention 36

Data Analysis 36

Chapter 4: Results and Discussion 43

Results 43

Frontal Cortex 43

Nucleus Accumbens 43

Conclusions 44

Future Directions 45

Intraperitoneal Studies 45

Molsidomine 45

Intranasal Nitroglycerin 46

References 53

VITA 55

List of Tables

TABLE 2.1: CALIBRATION SOLUTIONS 23

TABLE 3.1: RANDOMIZATION OF TREATMENT ORDER 38

TABLE 3.2: SUBCORTICAL COORDINATES 40

TABLE 3.3: ADVERSE OUTCOMES LEADING TO PREMATURE EXPERIMENTATION TERMINATION 41

TABLE 4.1: EXPERIMENTAL TRACING, ANIMAL 6 NG-10 48

TABLE 4.2: AUC OF TEST ARTICLES IN THE FRONTAL CORTEX 49

TABLE 4.3: AUC OF TEST ARTICLES IN THE NUCLEUS ACCUMBENS 50

TABLE 4.4: EXTRACELLULAR NO• LEVELS IN THE FRONTAL CORTEX FOLLOWING INTRAPERITONEAL ADMINISTRATION OF NO• DONORS 51

Table 4.5: EXTRACELLULAR NO• LEVELS IN THE NUCLEUS ACCUMBENS FOLLOWING INTRAPERITONEAL ADMINISTRATION OF NO• DONORS 52

List of Figures

FIGURE 1.1: STRUCTURE OF NITROGLYCERIN 11

FIGURE 1.2: NEURONAL SIGNALING PATHWAYS OF NITRIC OXIDE 12

FIGURE 1.3: HUMAN NASAL CAVITY 13

FIGURE 1.4: OLFACTORY NERVE AND OLFACTORY REGION CELL TYPES 14

FIGURE 2.1: MEA SIZE AND DESIGN 20

FIGURE 2.2: MPD AS AN EXCLUSION LAYER 21

FIGURE 2.3: Ag/AgCl REFERENCE ELECTRODE COATING 22

FIGURE 2.4: CALIBRATION SET-UP 24

FIGURE 2.5: NITRIC OXIDE CALIBRATION GRAPH 25

FIGURE 3.1: DORSAL SKULL VIEW 39

FIGURE 3.2: EXPERIMENTAL POSITIONING 42

Chapter One: Introduction and Outline

Nitric oxide

Nitric oxide (NO•) was recognized as a messenger molecule and chemically identical to endothelium derived relaxing factor (EDRF) in 1988 (Tassorelli et al., 1999)(Garthwaite et al., 1988). This substance was known to cause vasodilation in the vasculature but the structure was unknown until 1988. Substances that act as nitric oxide donors, such as nitroglycerin and molsidomine, have been utilized to treat angina pectoris and myocardial infarctions due to these drugs abilities to lower blood pressure by relaxing blood vessels, allowing them to expand. Since then, nitric oxide's cellular pathways, physiological roles and pathological associations in the brain have been elucidated. NO• has been implicated in disorders such as schizophrenia (Bernstein et al., 2005), drug addiction (Herman, 1995), and cancer (Choudhari et al., 2013). While further research is necessary to fully understand the role of NO• in these disorders, the role of nitric oxide in excitotoxicity, long term potentiation (LTP) and synaptic plasticity is well understood (Hardingham et al., 2013). One of the most well understood roles of NO• is in long-term potentiation (LTP) and synaptic plasticity. This occurs via the activation of NMDA channels and postysnapic influx of Ca^{2+} that increases production of NO• (Hardingham et al., 2013). NO• then acts as a retrograde secondary messenger and strengthen the synapse, which is the cellular basis of learning.

Nitric oxide is unique as a transmitter in the CNS in that it is membrane-permeable and cannot be sequestered in synaptic vesicles or spatially constrained by the synaptic cleft, as it can rapidly diffuse away from its source site across cell membranes (Tassorelli et al. 1999). For this reason it is not considered to be a neurotransmitter under the classical definition that restricts neurotransmitters to chemical substances that are generated in advance, stored in synaptic vesicles and, when released, diffuse and bind post-synaptically. The half-life of nitric oxide, *in vivo*, was found to be on the order of half a second, which is relatively short when compared to the traditional neurotransmitter dopamine, that has a half life of 2 minutes (Santos et al., 2011). However, there are still thought to be two modes of transmission that NO• takes part in; local

signaling, in the retrograde direction, and volume-type transmission wherein multiple synchronous sources summate spatially (Garthwaite, 2018).

Synthesis and signaling

One way in which NO• is synthesized in the brain is by neuronal nitric oxide synthase (nNOS) via increase in intracellular calcium (Ca^{2+}) that follows the activation of N-methyl-D-aspartate (NMDA) receptors (Santos et al., 2011). Glutamate, an excitatory neurotransmitter, binds to and activates NMDA receptors to cause a localized increase in calcium through the opening of calcium ion channels. Neuronal NOS is a calcium dependent enzyme and synthesizes NO• from L-arginine (Garthwaite, 2018). While nNOS and epithelial derived nitric oxide synthase (eNOS) are dependent on calcium for activation, inducible nitric oxide synthase (iNOS) is not. Ca^{2+} has such an affinity for iNOS that its activity is not modulated by calcium signaling but rather is mediated by cytokines (Hardingham et al., 2013). Additionally, the three types of NOS isoforms are found in different areas of the brain. nNOS has been found in 1-2% of neurons while eNOS has been localized to endothelial cells in the vasculature and to a small portion of neurons in the hippocampus. Finally, iNOS has not been found to be expressed in the healthy brain but has been seen in microglia and astrocytes following brain injury (Tassorelli et al., 1998). It is important to note that there is no consistent pattern of expression of NOS in terms of being localized to excitatory over inhibitory neurons. However, in some regions of the brain, such as the cerbellum, nNOS is found in a majority of the cells (Garthwaite, 2018).

Nitric oxide's mechanisms of action is known to be mediated through soluble gaunylyl cyclase (sGC). SGC, a heterodimeric enzyme consisting of one alpha and one beta subunit, is the most sensitive receptor of NO• (Hardingham et al., 2013). Two isoforms of alpha subunit exist and have differing regional expression. For example the alpha1/beta1 heteromer is dominate in the caudate-putamen and nucleus accumbens, a nucleus of interest in this study. The mechanism of action of activation of sGC by NO• is mediated by conformational changes via the binding at the heme site which enables sGC to convert GTP to cGMP (Hardingham et al., 2013). The receptor does this with incredible 10,000 fold selectivity of NO• over O_2, despite the two molecules having similar anatomical structures. cGMP is then able to effect cGMP-activated

protein kinases such as protein kinase G (PKG), initiating further downstream signaling events including phosphorylation of effector proteins (Hardingham et al., 2013). A depiction of the signaling pathways for NO• is found in **FIGURE 1.2**. Its important to note that signaling mechanisms may be tissue specific and are not fully understood. Factors such as nNOS concentration and local tissue media likely play a large role in the tissue specific role of nitric oxide (Garthwaite, 2018), (Santos et al., 2011).

Decay and removal

The half-life of NO• in Wistar rats, via carbon-fiber microelectrodes and ceramic-based microelectrode arrays, was determined to be 0.42 to 0.75 seconds (Santos et al., 2011). The ways in which NO• consumption impose this short half-life remains unclear. While several enzymes may contribute to NO• consumption in the brain, such as oxygen, cytochrome c oxidase, superoxide radical and cytochrome-P450 oxidoreducatse, the full mechanism of CNS NO• inactivation remains uncertain (Santos et al., 2011).

Through the understanding that nitric oxide follows an apparent first-order decay rate, Santos et al. was able to study the role of red blood cells in NO• consumption through inducing hemorrhagic shock in wistar rats. One hour of progressive blood withdrawal resulted in cardiac arrest. During the hemorrhage, *k*, the first-order decay rate constant, was found to decrease. The average decrease was 53+/-4.6%, which was twice the decrease seen in anoxia conditions. These results suggest that circulating RBCs have a major role in governing nitric oxide dynamics in the brain and likely act as the largest NO• sink in the vasculature. This study additionally reported on the role of the vasculature in a neuroprotective auto regulatory loop whereby local ischemia causes an increased concentration of NO•, which causes vasodilation which would decrease ischemia and reduce the level of NO• that, in high concentrations, can be neurotoxic.

Scavenging of NO• by erythrocytes suggest NO• can easily diffuse through the vascular wall (Santos et al., 2011). NO• small size and hydrophobic nature has supported the notion that NO• diffuse freely in tissues. (Lancaster, 1997). While most molecules are retained in extracellular space due to tortuosity, Santos et al. 2011 found that nitric oxide is not constrained in the extracellular matrix in the same way most CNS signaling molecules are. Electrode

recordings in agarose gel and *in vivo* in the rat brain found that NO• has a fast diffusion coefficient of 2.2 x 10^{-5} cm^2/s and additionally suggested a role of cell membranes and hydrophobic structures as facilitating NO• diffusion.

The mechanism in which NO• is cleared by RBCs is well understood through the binding of NO• to deoxygenated hemoglobin (Gow et al., 1999). NO• acts to nitrosylate hemoglobin thiols or react with free superoxide molecules in solution. The enzyme superoxide dismutatse (SOD) acts to eliminate superoxide in RBCs, increasing the concentration of S-nitrosohemoglobin and nitrosylated hemes. SOD concentration is therefore able to regulate the production of nitrosylated hemoglobin thiols. This pathway of NO• inactivation allows RBCs and hemoglobin to act as a main regulator of NO• levels *in vivo* (Gow et al., 1999).

Nitroglycerin

Nitroglycerin, as depicted in **FIGURE 1.1**, has been utilized to treat angina pectoris and myocardial infarctions since the 1970's due to its vasodilating effects. Vasodilation leads to increased coronary blood flow and reduction in cardiac pre- and post loads, treating the aforementioned disorders. Nitroglycerin acts via the formation of the reactive intermediate nitric oxide, who's cellular effect is described in the section titled "Nitric Oxide". Nitroglycerin is small, non-polar and highly lipophilic and, consequently, should have good permeability of the blood brain barrier (BBB) to enter the CNS. While the complete mechanisms in which nitroglycerin is converted to NO• in the brain are unknown, it is understood that the enzymes glutatione-S-transferase and cytochrome P450, which are involved in biotransformation of organic nitrates, are responsible for synthesis of NO• in the brain parenchyma (Tassorelli et al., 1999). Studies have demonstrated that nitroglycerin is biotransformed mainly by sulphydryl-dependent enzymatic processes but can additionally be synthesized by sulphydryl-dependent non-enzymatic processes. Interestingly, application of nitroglycerin onto brain nuclei causes an increase in the neuronal discharge rate. While, neurologically, nitroglycerin has been demonstrated to induce migraines, it shows promise as a nitric oxide supplement to potentially benefit disorders such as as drug addiction and schizophrenia. Additionally, nitroglycerin has

already been FDA approved, minimizing the amount of time and financial resources that drug researchers have to put forward in order to yield potential new medications.

Frontal Cortex

The frontal cortex has been implicated in many functional roles within the brain such as decision making, language skills, emotion cognition and general consciousness (Teffer, 2012). The frontal region of mammalian brains is functionally unique in that it is not defined by a predominate input from any sensory system. Other cortical regions such as the occipital lobe and parietal lobe can be attributed to sensory input of vision and proprioception, respectively (Klob, 1984). The frontal cortex has been associated with conditions like schizophrenia and drug addiction through the mesocortical pathway (Ekhtiari & Paulus, 2016). This pathway is a tract of dopaminergic neurons that connects the ventral tegmental area (VTA) with the pre-frontal cortex (PFC). This pathway is highly associated with cognition and executive function. Increased activation of this pathway is associated in drug addiction (Ekhtiari & Paulus, 2016). Conversely, dysfunction of this pathway has been found to be implicated in the negative symptoms of schizophrenia. Interestingly NO• has been implicated in pathologies of the frontal cortex through studies such as Reif et al., 2006. This study found that a functional SNP in the promoter region of nNOS is associated with schizophrenia and a worse frontal brain function.

Animal models, especially the use of rats, for research into frontal cortex injury and function have been widely accepted in the research community. Despite large differences in the relative volume of the frontal cortex across species of mammals, there appears to be a largely conserved functions of the region (Kolb, 1984). This conservation of function is seen through studies that found both lesion and insult to the prefrontal cortex of both primates and rodents yielded similar sets of symptoms. These symptoms include poor performance on spatial learning tasks, reduced facial expression and impaired performance on tasks requiring changes in behavior (Kolb, 1984). These functional similarities suggest sufficient levels of translatability from rat studies to humans to support rat models of frontal cortex research.

Nucleus Accumbens

The nucleus accumbens (NAc) has long been dubbed the "pleasure center" of the brain. This nucleus was first recognized as anatomically distinct from the more dorsal striatum by Lennard Heimer in 1975. The role of the NAc has since been further elucidated and it is better understood as a nucleus that aids in obtaining and directing attention towards motivationally relevant goals by promoting behaviors that increase the likelihood of obtaining rewards (Floresco, 2015). The NAc is highly connected to other subcentral structures. It received inputs from the prefrontal cortex, basolateral amygdala, hippocampus and VTA. Outputs of the NAc include the ventral pallidum, hypothalamus and midbrain (Floresco, 2015). This strong interconnectedness allows the region to integrate many different inputs to direct behavior towards attaining potential rewards.

The NAc has been associated with pathologies such as schizophrenia and drug addiction through the mesolimbic pathway. The mesolimbic pathway is a tract of dopaminergic neurons that connects the ventral segmental area with the nucleus accumbens (Ritz & Kuhar, 1993). This pathway is highly associated with human motivation, emotion and reward and its dysfunction is associated with the positive symptoms of schizophrenia and drug addiction (Floresco, 2015). Drug abuse is thought to cause increased dopamine neurotransmission in the mesolimbic pathway, which reinforces the behavior of drug administration and contributes to the addictive properties of many drugs (Ritz & Kuhar, 1993). Additionally, the nucleus accumbens, along with other structures within the striatum, has been found to have some of the highest concentrations of nNOS in the human brain and, consequently, is an area of intense interest in NO• research and pathologies (Bernstein et al., 2005).

Intranasal Drug Administration

Nasal administration of drugs was perviously reserved only for local treatment of disorders such as nasal allergy, nasal congestion and infections. Although the effect of nasally administered drugs on the CNS has been recognized since before the cocaine boom of the 1980's, it wasn't until more recently that pharmaceutical drug companies have developed nasally administered to treat CNS disorders. Examples include the use of intranasal (IN) morphine and

ketamine, to treat pain, and apomorphine to treat erectile dysfunction. This route of administration is expanding due to the limitation of off target effects and rapid onset (Illum, 2003).

Recently, drug development has branched into nasally administered vaccines, such as influenza and the treatment of neurodegenerative disorders like Alzheimer's disease (Illum, 2003). Through IN administration, researchers have reversed neurodegeneration and rescued memory in a transgenic mouse model of Alzheimer's (Hanson & Frey, 2008). Additionally, IN insulin-like growth factor-I and erythropoietin have been shown to protect the brain against stroke in animal models (Hanson & Frey, 2008). Additionally, IN insulin has been shown to improve memory, attention and function in patients with Alzheimer's disease without altering blood glucose (Hanson & Frey, 2008). Here, I will discuss the ways in which drugs administered via the nasal cavity are able to enter the CNS without crossing a selective filter such as the blood brain barrier, the pros of nasal administration and considerations for the use of IN drugs in animal models such as rats, which were utilized in this study.

Intranasal (IN) drug delivery has been utilized to circumvent the blood brain barrier (BBB) that usually inhibits the transport of large, polar, hydrophilic molecules into the CNS (Hanson & Frey, 2008). The BBB, at the cellular level, is generally referred to as a neuro-vascular unit. This is comprised of endothelial cells of brain capillary walls, astrocyte end-feet that surround the capillaries and pericytes (Hanson & Frey, 2008). These cell structures help to block the import of unwanted compounds found in circulating blood through tight junctions, selective protein transporters and even cassette protein transporters that can export unwanted compounds once they have entered the CNS.

Pros of IN administration over general systemic administration of compounds includes convenience, safety, cost and limitation of off-target effects. IN delivery limits the amount of the compound that enters the systemic circulation (Hanson & Frey, 2008). This minimizes off-target, possible negative side effects and the potential need to co-dose with peripheral inhibitors, as seen in the case of LDOPA and its peripheral inhibitor Carbidopa. An example is that of IN administered insulin which does not significantly effect blood glucose levels, demonstrating a

lack of off-target effects of IN administered drugs (Hanson & Frey, 2008). However, it is important to note that when drugs enter the nasal cavity, a portion still enters the blood stream and can affect tissues and organs, causing off target effects. A portion of the drug in the blood stream may be able to traverse into the CNS by penetrating the BBB. The percentage of compound that will successfully penetrate the BBB is dependent on the properties of the compound. Large molecular weight polar drugs such as peptides and proteins have relatively low permeability, generally no more than 1% for peptides and 10% for small polar drugs (Stenslik et al., 2015). Lipophilic drugs are generally well absorbed from the nasal cavity and boast bioavailability rates approaching 100%. One example of such a compound is IN fentanyl, that boasts an impressive bioavailability of ~80% (Illum, 2003).

The olfactory nerve pathway has long been described as the main pathway to the CNS but recently the role of the trigeminal nerve in providing a direct connection with the CNS has been elucidated. Both nerves innervate the nasal cavity and consequently provide a direct connection to the CNS. A depiction of the innervation of the nasal cavity is seen in **FIGURE 1.3**. It is interesting to note that the trigeminal pathway has been associated with drug delivery to more caudal brain regions and the spinal cord when compared to the olfactory nerve pathway. For a drug to reach the CNS from the nasal cavity it has to transverse the nasal olfactory epithelium and, depending on the path taken, the brain's arachnoid membrane (Illum, 2000). There are three suggested pathways that a drug can take to cross the olfactory epithelium, pictured in **FIGURE 1.4.** First, the transcellular pathway utilizes receptor mediated endocytosis, fluid phase endocytosis or passive diffusion to allow drugs to cross the olfactory region's cellular layer, specifically sustentacular cells (a type of support cell) (Illum, 2000). Next, paracellular transport is possible via tight junctions found between sustentacular cells and olfactory neurons. Finally, there is transport of compounds by the olfactory nerve pathway. In this mode the drug is taken up by a neuron via endocytosis or pinocytosis and then transported by axonal transport to the olfactory bulb. This pathway is thought to be relatively slow compared to the extracellular delivery pathways (Illum, 2000).

There are many considerations to take into account with IN drug development. The nasal mucociliary clearance system has a half-life in the order of 15-20 minutes (Illum, 2003). This can decrease the absorption and bioavailability of the compound in the CNS, especially for drugs that are not easily absorbed across the nasal membrane (Illum, 2003). This issue can be resolved, in part, through the implantation of co-administered compounds that effect nasal absorption. These compounds, which include bile salts, work by either delaying the mucociliary clearance or increasing paracellular transport by opening the tight junctions between the epithelial cells (Illum, 2003). Compounds such as starch and chitosan have been shown to slow mucociliary clearance and consequently increase the bioavailability of the drugs in the CNS (Illum, 2003).

While no compound was co-administered in this study, the chemical properties of nitroglycerin, the nitric oxide donor utilized in this study, shape the compound as a potentially membrane permeable drug. Nitroglycerin has a relatively low molecular weight, is non-polar, and lipophilic, which is expected to enhance its ability to diffuse through sustentacular cells in the olfactory region of the nasal cavity (Tassorelli et al., 1999). A pro for the utilization of nasal administration of nitroglycerin is the potential limitation of off-target effect of peripheral vasodilation, which results in decreased blood pressure.

It is important to take into consideration the species difference between humans and animal models of IN administration of drugs. The olfactory region of mouse, rat and non-human primate animal models cover a much larger proportion of the nasal cavity as compared to humans. Furthermore, in rat IN studies, the rat is commonly placed on its back during the study, which can increase the contact of the drug with the olfactory region. While this position was not used due to the MEA head-cap and FAST system attachment, the modified prone position that was utilized could potentially increase the amount of contact the test articles, nitroglycerin and miglyol, had with the olfactory region of the animal. These two considerations foster rat model studies as yielding more pronounced olfactory transport of drugs than in humans (Illum, 2000).

Thesis Outline

This study was utilized to determine the feasibility of measuring extracellular NO• in the CNS while administering a NO• donor, nitroglycerin, nasally and determining the amplitude and

kinetic time course effects of a nasal delivered NO• donor in two rat brain areas, the frontal cortex and the nucleus accumbens. This section, Chapter One, covered the relevant background and current understanding of the synthesis, signaling and clearance of nitric oxide in the mammalian brain. Chapter Two will cover the use of microelectrode arrays (MEAs) as a measurement of nitric oxide in the extracellular space in two aforementioned subcortical structures. This includes a look into MEA fabrication, mPD exclusion layer coating and calibration carried out prior to electrode implementation. Chapter Three will delve into the experimental design, materials, surgical methods, experimental methods and statistical analysis used in this study. Finally, Chapter Four will cover the main findings of this study, considerations, and future directions.

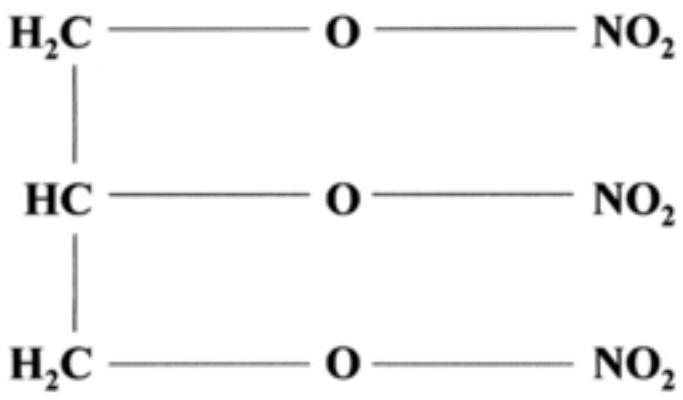

FIGURE 1.1: STRUCTURE OF NITROGLYCERIN

Shown above is a depiction of nitroglycerin as seen in Tassorelli et al., 1999. It is easy to see how, when present in solution, nitroglycerin is non-polar with all three nitrate groups canceling each other out to leave a relatively non-polar compound free of large dipole interactions. This molecule is highly lipophilic and has a relatively low molecular weight.

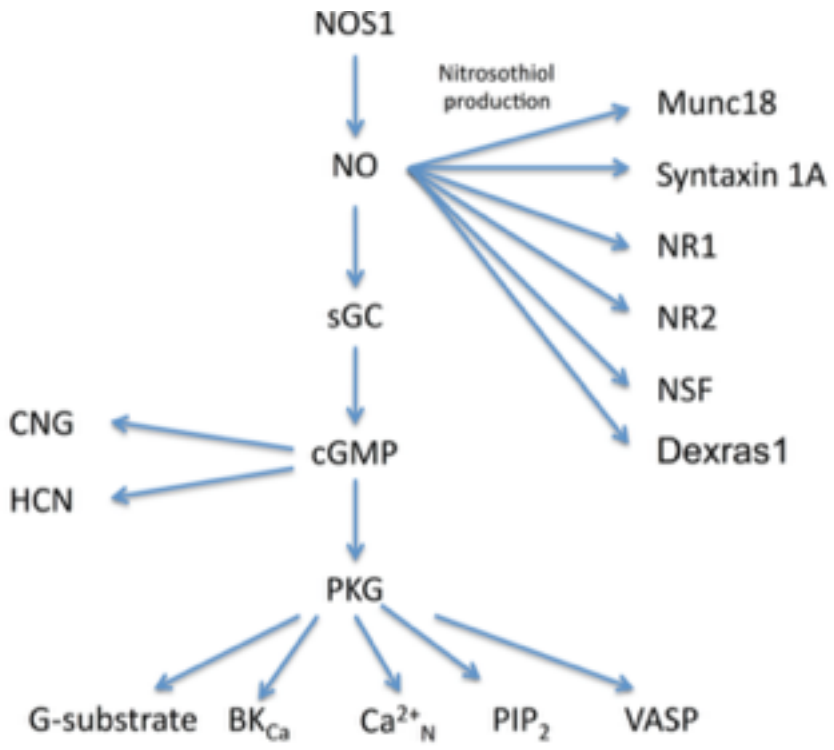

FIGURE 1.2: NEURONAL SIGNALING PATHWAYS OF NITRIC OXIDE

Seen above is a schematic of the signaling pathway of nitric oxide as seen in Hardingham et al, 2013. This image depicts the signaling cascade from nNOS, shown here as NOS1, to the production of NO•, binding to sGC and production of cGMP that can cause multiple down stream effects. Not discussed in the corresponding section is the role of nitrosothiol groups in maintaining neuronal homeostasis and pre-synaptic plasticity.

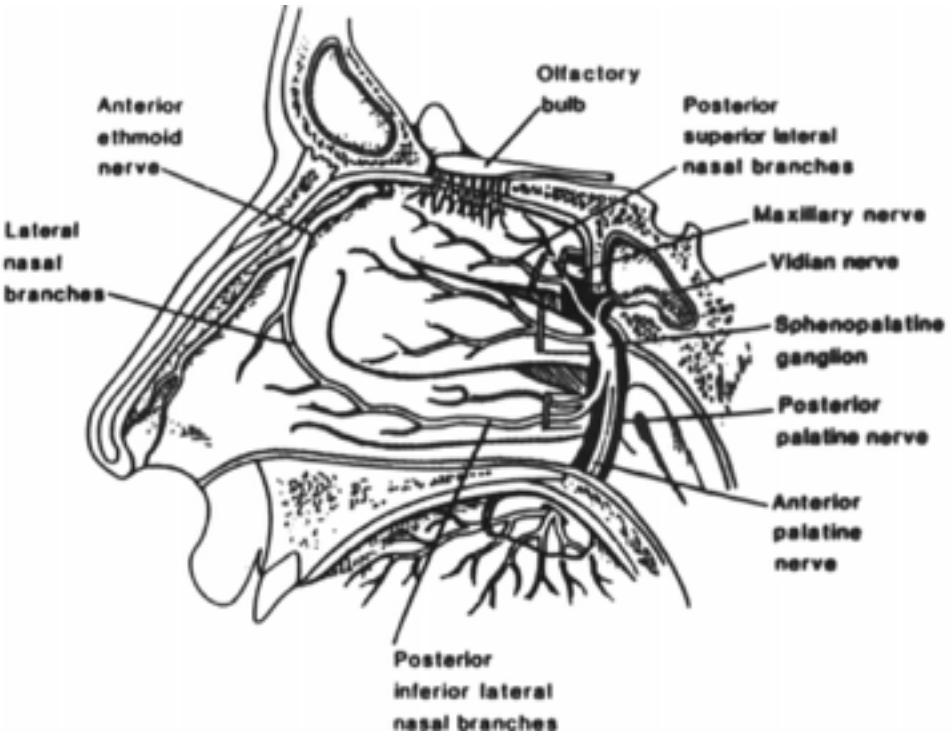

FIGURE 1.3: HUMAN NASAL CAVITY

The image above is depicted in Illum et al. 2000. This image depicts the olfactory bulb and its associated sensory neuron bundles that penetrate through the cribriform plate to the nasal cavity. This figure also depicts the high degree of innervation throughout the nasal cavity and facial region. This betters the visual understanding of the role that trigeminal nerve plays in nasal drug delivery alongside the olfactory nerve. It is also helpful to note the proportion of the nasal cavity that the olfactory region (below the olfactory bulb) occupies, as this is discussed in the considerations section of “Intranasal Drug Administration”.

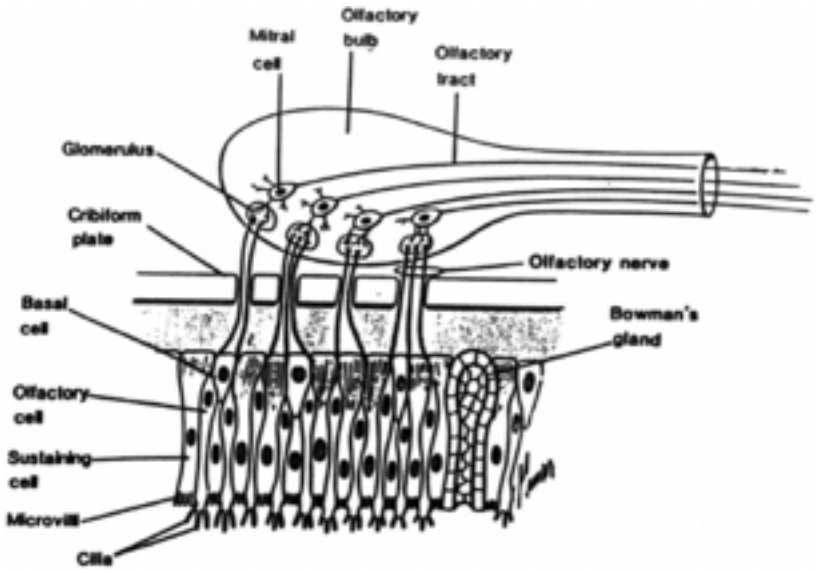

FIGURE 1.4: OLFACTORY NERVE AND OLFACTORY REGION CELL TYPES

Depicted are the various types of cells that support the olfactory region of the nasal cavity. Support cells, seen here as sustaining cells, are an integral part of the transcellular and paracellular pathways of IN drug uptake. Olfactory receptor cells are bipolar neurons which are seen here as "olfactory cell". These cells give rise to a single non-myelinated axon which forms large bundles with other olfactory cells and penetrate through the basal membrane and, subsequently, through the holes in the cribriform plate. These fibers then synapse in the glomeruli, which reside near the surface of the olfactory bulb (Illum et al., 2000).

Chapter Two: MEA Electrochemistry, Fabrication and Calibration

MEA Fabrication

Enzyme-based multisite microelectrode arrays are mass fabricated using photolithographic methods. This allows for mass production of reproducible recording surfaces as small as 5-10 µm (Hascup et al. 2006). A 2.5 cm x 2.5 cm x 125 µm thick ceramic wafer serves as a common substrate for the MEAS. Ceramic is used since it reduces the cross-talk from adjacent connecting lines and is strong and rigid (Hascup et al. 2007). Thin Films Technology, Inc., (Buellton, California) was the manufacturer of the four channel MEAs utilized in this study. Copper wires are soldered onto the paddle, one for each corresponding platinum (PT) recording site. Gold sockets are soldered to the other ends of the copper wire, which are inserted into a miniature black connector along with a miniature silver/silver chloride wire. Five-minute epoxy is applied to hold the apparatus together and keep the ceramic tip of the MEA parallel to the miniature black connector for stereotaxic placement. At this point, the entire apparatus is now referred to a pedestal MEA (Hascup et al. 2007). The MEAs were delivered to the Gerhardt lab pre-fabricated, only requiring reference electrode coating, mPD coating and calibration prior to being utilized in the study. An image of an MEA pedestal and rendering of the electrode tip can be found in **FIGURE 2.1**.

Solutions Used

Solutions used includes 0.05 M Phosphate Buffered Saline solution (PBS lite). The pH of the solution was tested and determined to be a desired 7.4.5mM. m-Phenylenediamine (mw 181.1 Aldrich Chemistry) was made fresh daily due to the solutions tendency to oxidize within a few hours of synthesis. Additionally, 20 mM sodium nitrate solution and 8.8 mM hydrogen peroxide, 2.0 mM dopamine were used.

diethylenetriamine (DETA)/ nitric oxide adduct

A 20 mM solution of DETA was utilized. This solution takes at least an hour to generate a stable concentration of NO• so the solution was allowed to sit for the minimum amount of time to generate a final NO• concentration of 0.2 mM before being used in a calibration experiment.

5 mM m-Phenylenediamine

5mM m-Phenylenediamine (mw 181.1 Aldrich Chemistry) was made fresh daily due to the solutions tendency to oxidize quickly (within a few hours of synthesis). First, nitrogen gas was bubbled through 100 mL of 0.05 M PBS solution for no less than 20 minutes. See PBS lite solution recipe above. Then 0.0905 grams of mPD (Sigma-Aldrich) was added to the 100 mL of PBS. This solution was inverted in the volumetric flask three times to mix. Solution was temporarily stored with paraffin film (Parafilm) until used to coat the MEA electrodes.

mPD Coating

5mM m-Phenylenediamine was made fresh daily as detailed in the "Solutions Used" section. A glass reference Ag/AgCl electrode, that is reserved just for plating, was placed in the beaker and attached to the Quanteon 20pA/mV headstage (Quanteon, Lexington, KY). The MEA was then attached to the headstage using the connector and the tip of the electrode was submerged in the mPD solution. Electroplater software was used (Quanteon, Lexington, KY). The P-P amplitude was set to 0.25, the offset was set to -0.5. Frequency was set to 0.05 Hz. This resulted in a wave pattern that generated three triangular waves per second. The Electroplater system was allowed to run for 15 minutes to sufficiently coat the electrode in mPD. The same electrode system was run in reverse chronoamperometry via the FAST system (Quanteon, Lexington, KY). The system was set to run at -0.55V vs. Ag/AgCl. This reverse current was utilized to partially remove some of the accumulated mPD. This process has been found to not negatively effect the role of the exclusion layer but simply boost nitric oxide selectivity (Friedemann et al., 1996). The mPD solution was exchanged for PBS and allowed to run for 5 minutes. After the completion of this reverse current, the MEA was removed from the headstage apparatus and stored at room temperature in a covered, light-proof container.

Ag/AgCl Reference Coating

While larger glass Ag/AgCl reference electrodes are suitable for mPD electropolymerization and microelectrode calibration, this reference electrode is too large for many biological applications. For this reason, a smaller Ag/AgCl reference electrode is fabricated and adhered to the head-cap of the MEA. In this section I will describe the process of coating this Ag wire with chloride (Cl). First, the ends of the silver wire were stripped of Teflon coating. The

head cap was then placed into a clamp and the exposed end of the wire was placed into a 1 M HCl saturated with NaCl. A Pt wire acts as the counter electrode and was also placed into the solution, not touching the silver reference electrode wire. Alligator clips, that were powered by a 9V DC adapter, were attached to the electrode head-cap and the end of the platinum wire. The applied potential then attracted Cl- ions to the silver wire to form AgCl, thus yielding the Ag/ AgCl reference electrode. This phenomena was observed as reactive bubbling on the surface of the Pt wire. Current was sustained until there was an absence of new bubble formation, which signaled the end of the reaction. This generally took less than one minute in time. A depiction of reference electrode coating is seen in **FIGURE 2.2.**

Calibration

Calibration is utilized to test substance selectivity and normalize the coated sites for self-referencing recordings. Using the FAST recording system, a nitric oxide donor (DETA) was the analyte of interest. MPD coating on the MEA, the exclusion layer, worked to select against measuring nitrate by physically blocking it from interacting with any of the four channels. Sodium nitrate was utilized as the interferent. Hydrogen peroxide (H_2O_2) was utilized as the positive control and displayed the sensitivity of the MEA. The analyte concentration was 0.2 μM and the interferent concentration was 250 μM. Recordings took place at 0.6V vs. Ag/AgCl applied voltage and recordings were measured at 100Hz. P200s and P1000s (Rainin micropipette), and corresponding 200mL and 1000mL pipette tips, were used during calibration as well as later during experimentation. Four compounds — an interferent (nitrate), analyte (nitiric oxide) and two test substances (DA and H_2O_2) — were applied to the PBS solution throughout the course of the calibration. A table of the order and volume of added solutions can be found in **TABLE 2.1.** All solutions were stored in a refrigerator at 5 degrees celsius.

A 50 milliliter glass beaker was filled with 40 mL of 0.05 M PBS solution. This beaker was placed in a plastic holder which rested upon a battery operated, portable magnetic stir plate (Cole and Parmer portable magnetic stirrer). A battery operated stir plate was used to reduce potential AC (60Hz) current that can affect the recordings. A magnetic stir bar was added to the PBS solution and was set to stir slowly to avoid the formation of a vortex in the solution. A glass

Ag/AgCl reference electrode is placed in the buffer solution. The microelectrode was attached to a 2pA/mV Quanteon headstage. The end of the Ag/AgCl reference wire is also plugged into the headstage. Finally, the microelectrode tip was partially lowered into the PBS solution (approximately a few millimeters). A photograph of the calibration system can be seen in **FIGURE 2.4**. After initial system settings were established on the FAST software, the recording system applied a potential of +0.6 V versus the Ag/AgCl reference to the microelectrode recording surfaces. The current was allowed to reach a stable baseline. This generally took anywhere from 10-15 minutes time. Once the baseline was achieved, it was 'marked' on the FAST computer system.

Following the establishment of a baseline voltage, 500 µl of nitrate was added for a final beaker concentration of 250 µM. When a new stable baseline was reached, the interferent was marked by the user. Next, three 40µl additions of 40 µM nitric oxide were added for final buffer concentrations of 40, 80 and 120 µl nitric oxide for a final concentration of 0.2 µM. Analyte marks were recorded after each addition to create the calibration curve. Following these three additions of analyte, 40 µl of 2 mM DA (2 mM, final beaker concentration) was added to the solution as a test substance and marked. Finally, 40 µl of 8.8 mM hydrogen peroxide was added to the solution to confirm microelectrode sensitivity and the addition was allowed to reach a new stable baseline and marked. A figure of the desired recording is found in **FIGURE 2.5**. After marking the second test substance baseline, the calibration was ended and resultant selectivity and sensitivity were analyzed. The MEA was removed from the apparatus and was stored at room temperature. The PBS solution that contained all four experimental solutions was discarded prior to starting another calibration.

Dopamine was utilized to further insure the integrity of the electrode and peroxide was used to examine the MEA over all responsiveness. The additions of test substances did not factor into calculating the standard curve for the analyte of interest since they followed the application of analyte. Chemicals used *in vivo* should be tested *in vitro* to ensure that they are not electrochemically active *in vitro* prior to its local application near the Pt recording sites during

experimentation. This ensures that *in vitro* or *in vivo* analyte concentration changes are from the analyte of interest rather than due to local application of drugs.

The calculations for selectivity ratios for nitric oxide over sodium nitrate, slope (microelectrode sensitivity for nitric oxide), limit of detection (LOD) and linearity (R^2) are found below. A poor linearity, calculated by R^2 is rarely seen with good microelectrodes. Since the microelectrode array fabrication procedure is highly reproducible, nitric oxide responses are extremely linear and resulted in linear regression curve fits with R^2 greater than or equal to 0.99. Sensitivity of the microelectrode refers to how well the electrode can measure the change in nitric oxide. The sensitivity is calculated by the slope of the three additions of nitric oxide. This number is used to equate a change in current to a change in nitric oxide concentration. The slope is also utilized to calculate limits of detection which we have designated as the most important criteria for determining if a microelectrode is satisfactory for use. We utilize limits of detection (LOD) to select microelectrodes because slopes can be misleading. LOD refers to the limit of detection for the microelectrodes defined as the analyte concentration that yields an electrode response that is equivalent to three times the background noise of the recording system. This is calculated by taking the root mean squared of the background signal multiplied by 3 then divided by the slope ((RMS background signal X 3)/slope of NO• signal). This is the lowest detectable change in analyte concentration that can not be attributed to noise, in other words the lowest detectable change that is significant. Microelectrodes with LODs that are lower than the response they expect to observe were selected. This is generally less than or equal to 1uM.

Selectivity refers to a ratio of the microelectrodes sensitivity to nitric oxide over interferents such as nitrate. It is calculated by dividing the nitric oxide slope by the nitrate slope. The slope of the interferent is simply one point, the single addition of nitrate as compared to the baseline signal, but this has been found to be sufficient for selectivity calculations. A microelectrode with a selectivity of 100:1 means that for every 100 molecules measured 99 are nitric oxide while only 1 is nitrate. A selectivity of 100:1 ensures that the microelectrode is 99% effective at blocking nitrate. Selectivity ratios of 100:1 or greater were ideal.

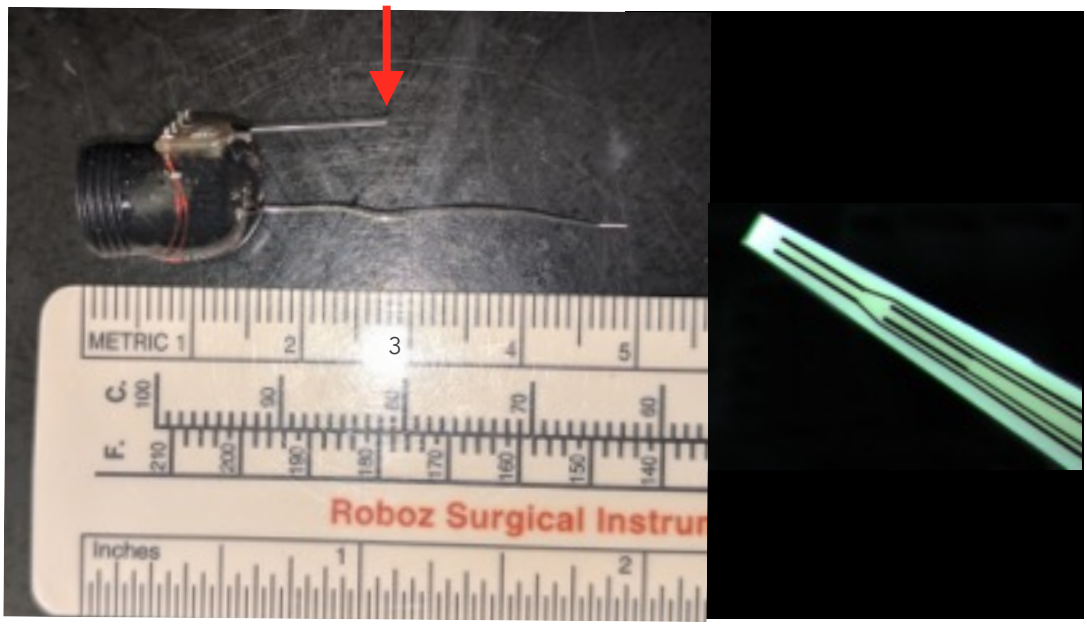

FIGURE 2.1: MEA SIZE AND DESIGN

Above is an image of the microelectrode array used in this study. Ceramic-based MEAs were assembled and prepared by Thin Films Technology, INC., (Buellton, California). In this image, the MEA is compared to a standard metric ruler shown in centimeters. The red arrow indicates the tip of the MEA that contains the four channel electrodes. The Ag/AgCl reference wire is seen extending to the 5 cm mark below the ceramic electrode tip. It is possible to see the whitened tip of the reference electrode that has undergone the reaction with HCl to yield a white Ag/AgCl coating on the end of the wire. An image of the four channels is shown to the right.

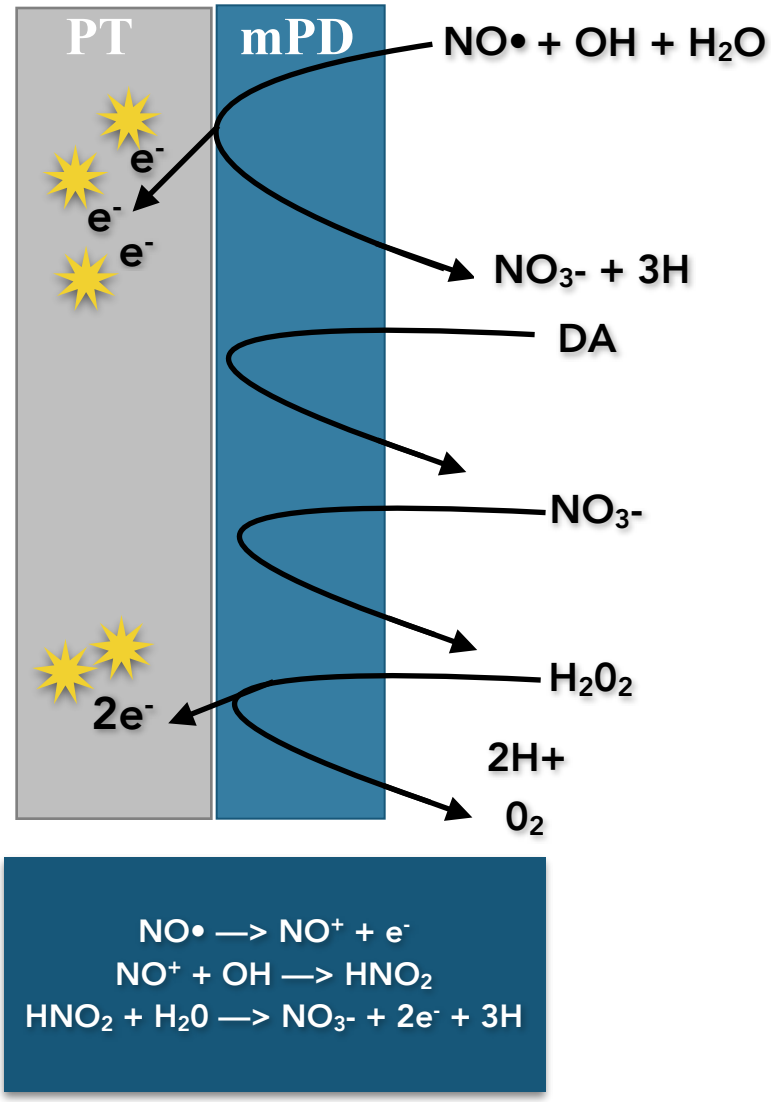

FIGURE 2.2: MPD AS AN EXCLUSION LAYER

MPD was utilized as an exclusion layer for the detection of dopamine *in vivo.* This image shows the selective exclusion of compounds such as DA and NO_{3-} , substances that could skew the accurate recording of NO• *in vivo.* Note that NO• and H_2O_2 are able to cross the mPD exclusion layer, reduce and donate one and two electrons, respectively, to the positively charged platinum (PT) sensor. The following balanced electrochemical reaction of the reduction of NO• on a metal surface, such as Pt, at a positive electrode potential. This reaction demonstrates that the oxidation of NO• in this experiment proceeds via a three-electron oxidation mechanism (Privett et al., 2010). A simplified equation is as follows: NO• + OH + H_2O —> NO_3- + 3e- + 3H

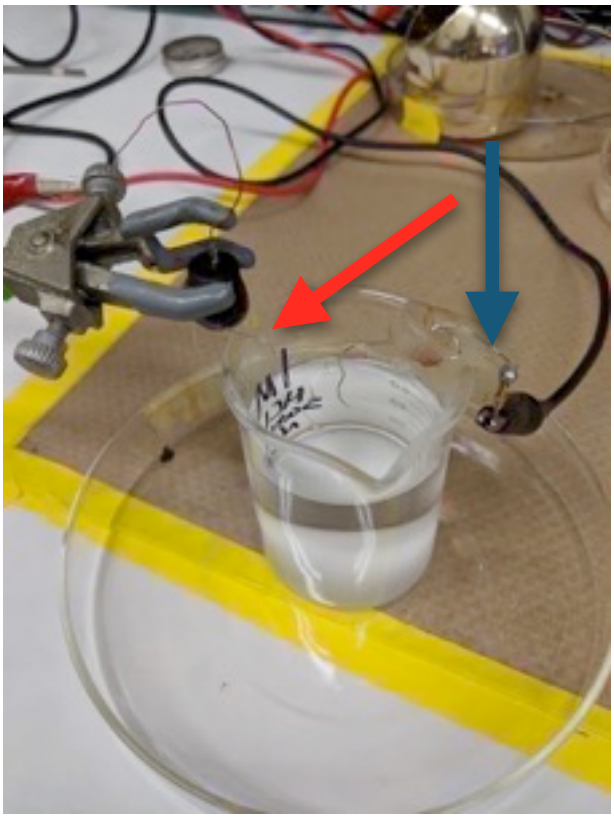

FIGURE 2.3: Ag/AgCl REFERENCE ELECTRODE COATING

Depicted is a beaker of 1 M HCL saturated with NaCl, the MEA electrode being held by a metal three-prong clamp (indicated by the red arrow, left) and a platinum (Pt) wire (indicated by the blue arrow, right). The MEA and Pt wire were attached to a 9V DC adapter fitted with alligator clips that were hooked to electrical wires as depicted. The reaction was run to yield an Ag/AgCl reference wire Once the reaction was run to completion and NO• further bubbling was observed on the Ag reference wire, the current was cut off. After coating, the ends of the silver wire were observed against a high-contrast black background to ensure that a bright, white Ag/AgCl reference wire was produced. MEAs were then returned to dark storage in boxes and were stored at room temperature.

Sequence of addition	Role	Volume/ Concentration	Solution	number of additions
1	Interferent	500mL/250uM	Nitrate	1
2	Analyte	40mL/6.2uM	Nitric Oxide	3
3	Test substance	40mL	DA	1
4	Test substance	40mL	H2O2	1

TABLE 2.1: CALIBRATION SOLUTIONS

This table depicts the order and volume of the solutions added throughout the course of electrode calibration. All agents were added after a baseline was established and "marked" on the FAST system. The first additive, nitrate, was added following a 15 minute stabilization period that allowed the electrode to establish a baseline under the applied voltage.

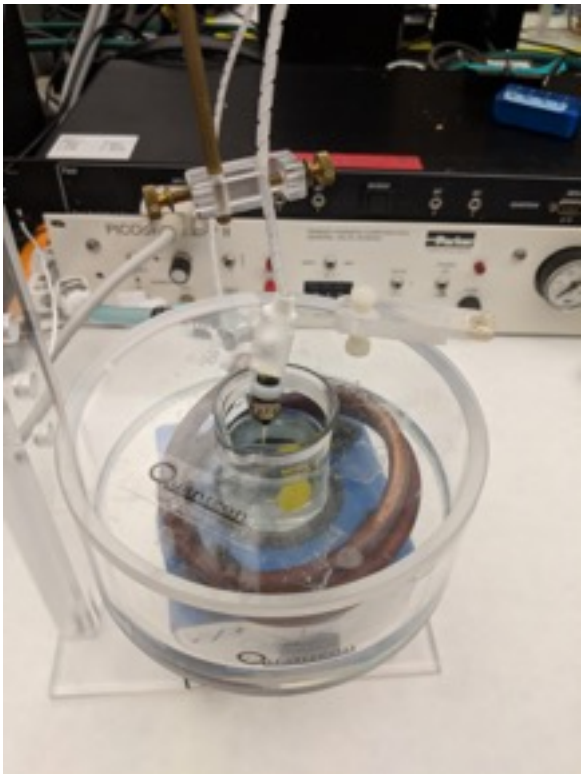

FIGURE 2.4: CALIBRATION SET-UP

Depicted above is the complete set-up of a calibration experiment. The plastic stand sits atop the battery powered magnetic stir platform. A 50mL beakers placed in the stand and filled with 40 mL of PBS lite solution. A miniature stir bar was added to the beaker and was utilized to circulate the added calibration compounds. The MEA is shown attached to the Quanteon 2pA/mV headstage, shown left. The silver reference electrode is shown on the right of the beaker and was attached to the reference attachment point on the headstage. Not shown is the connection to the FAST system, displayed on a desktop computer or the test compounds utilized during a calibration.

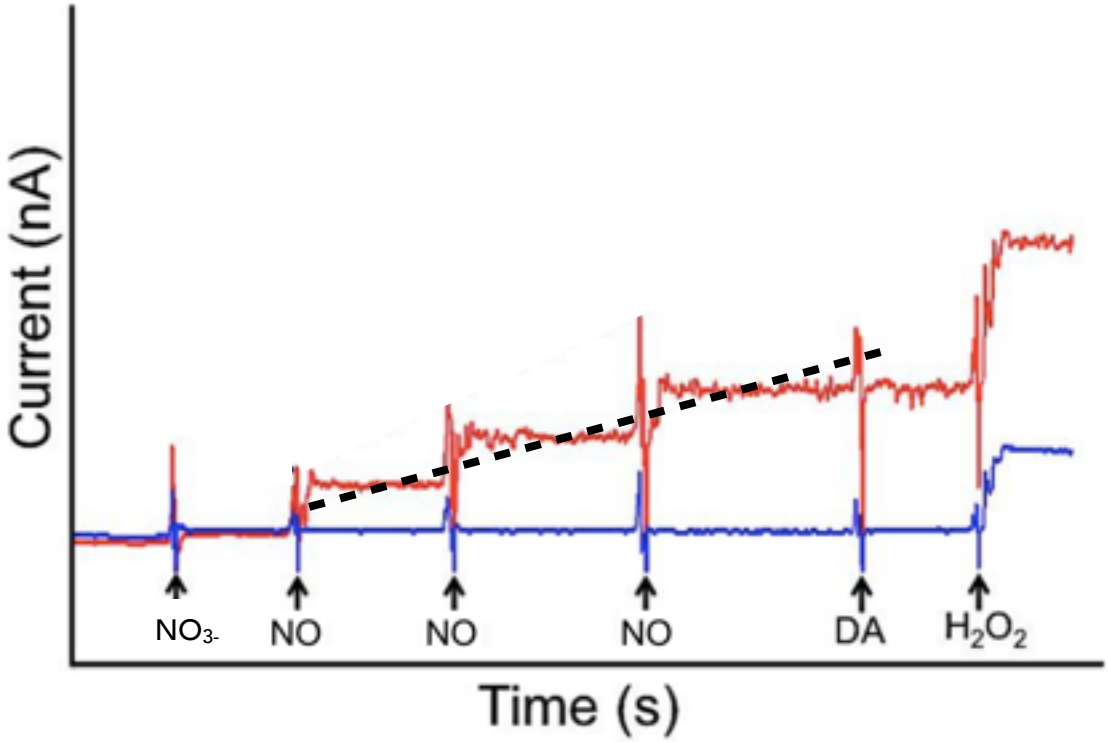

FIGURE 2.5: NITRIC OXIDE CALIBRATION GRAPH

This image was adapted from Hascup et al. 2006. The additions follow the order and volume noted in **TABLE 2.1.** This graph depicts the desired current observed from the subsequent additions of analytes over time. Note the lack of response after the addition of nitrate (denoted NO_{3-}). This is followed by three 40ml additions of the nitric oxide solution (NO). The dashed line indicates the slope of the analyte addition, showing compounding activation with each addition. The sensitivity of the microelectrode is inferred by the slope of the three analyte additions. The graph shown here has strong linearity and correlation between subsequent additions and detection of NO.

Chapter Three: Materials and Methods

Animals

A total of 10 (5 per brain region) research naïve male Wistar rats (F344) 1-2 months old weighing ~150-175 (Envigo) were needed for this study. Upon arrival at the University of Kentucky, individual cage-card and research chart were created and the animals were allowed to go through a standard acclimation/quarantine period while being housed in the DLAR facility. After the 7 days acclimation period animals were implanted with an electronic ID transponder.

The Wistar rat was chosen as the test system because of its established usefulness and acceptance as a rat strain. It is also the phylogenetically lowest species that provides adequate size, tissue and anatomy for the proposed studies. The number of animals used is the minimum necessary to obtain scientifically valid results. The total number of animals used in this study was 14, not 10, due to varied adverse outcomes that resulted in animals not completing the full three-part experiment. The study does not unnecessarily duplicate any previous work and alternatives to the use of live animals have been considered. Procedures used in this study have been designed to avoid or minimize discomfort, distress or pain in the animals. Animals that experienced severe chronic pain or distress that cannot be relieved would have been painlessly euthanized in consultation with the University of Kentucky veterinary staff and Study Director. The Study Sponsors would have been advised by the University of Kentucky in a timely manner of all circumstances that could have lead to this action.

Experimental Design

Two sets of *in vivo* electrochemical studies with 5 rats per arm (10 animals total) were carried out in order to evaluate the effects of nasal administration of NO• donor on extracellular NO• levels in 2 brain regions, the nucleus accumbens and frontal cortex. Each animal (n=10, 5 per brain region) received 3 treatments.

Due to the nature of these experiments and analyses, it was expected that the experiments be conducted for 3 weeks per animal (2 animals per week on study) with analyses performed on the data after completion. We estimated that the in-life of the recordings would span a total of 14 weeks and final analyses, histology and data analyses would take an addition 4-6 weeks; total

study in-life was estimated to be 24 weeks (6 months) including study start-up, which involves animal protocol approvals. The timeline was adjusted as study modifications were needed throughout the course of experimentation (when requested and approved by the study sponsor in consultation with the testing facility). All efforts were taken to maintain the study timeline, although secondary to any needed actions to maintain data quality and reproducibility.

Randomization and Blinding

Animals were randomly assigned into 2 groups (each brain region). Animals received placebo (negative control) and NO• donor (nitroglycerin at 2 different doses) and the test and control articles labeled A, B and C were administered via nasal administration such that Study 1 and Study 2 had a total of 10 animals that received the 3 treatments. Test and control articles, although identified alphabetically A, B and C by label, are coded by the study director so that experiments and analyses are performed with study staff blinded to the test groups. All animals received all three treatments, following the randomization scheme depicted in **TABLE 3.1.**

Test and Control Articles

The sponsor provided the NG formulations. The Study Director transferred materials to vials and prepared the saline and SNP solutions daily. The Study Director provided the 3 solutions (blinded) labeled A, B and C to the PI on the day of use.

Recipes:

A) Negative control (Miglyol)

B) Nitroglycerin (NG) 50 mg/ml (dissolved in Miglyol); 15 mg/kg

C) Nitroglycerin (NG) 50 mg/ml (dissolved in Miglyol); 10 mg/kg

(Nitroglycerin solution dissolved in Miglyol, 50 mg/ml - Novasep)

Test and control articles were stored as indicated by Novasep Synthesis.

Any residual test and control articles were stored at 5 degrees C in a refrigerator until after the final report has been signed/approved by the study director in consultation with the study sponsor, at which time residual samples may be discarded. The weight of the animals, on average, was slightly higher than the originally anticipated maximum value of 400 grams. Animal weight during experimentation ranged from 366-454 grams. The concentration of the test article was

adjusted accordingly by the study director to ensure the same volume of TA was delivered during experimentation.

Nasal Administration

The test and control articles were administered via nasal delivery with animals under isoflurane sedation, as described in Stenslik et al., 2015. Administration was via P200 micropipette tips. Further information and considerations of intranasal administration can be found in the corresponding section.

Controls

Controls are intended to show the effect of procedure or experimental design in the absence of the agent of interest. In this study, the control was Miglyol.

Husbandry and Veterinary care

The procedures described in this section were performed in accordance with the appropriate standard operating procedures in use by the University of Kentucky Division of Laboratory Animal Resources (DLAR). The animals were given an acclimation period of approximately one week. All adverse consequences resulting from administration of the test article and collection procedures as well as subsequent treatments provided by a qualified member of the veterinary staff were documented in the study records. While adverse consequences are described in the section labeled, "Adverse Outcomes", no subsequent treatments were provided by a member of the veterinary staff and consequently not recorded.

Animal Housing

All animals in the study were housed in the University of Kentucky DLAR facility, which is fully accredited by the Association for Assessment and Accreditation of Laboratory Animal Care (AAALAC). While on study, the animals were housed in plastic boxes and maintained on a 12-hour light/12-hour dark cycle in temperature-controlled and humidity-controlled rooms, ranging approximately from 64˚F to 84˚F and 30% to 70%, respectively. Each housing unit was identified with a cage card indicating, but not limited to: animal ID number, species, sex, vendor and IACUC protocol number. A variety of toys were provided to the animals for enrichment.

Dietary materials

Each animal was fed a standard, commercial diet *ad libitum*. Municipal tap water, purified by reverse osmosis was available *ad libitum* via an automated watering system. Additionally, animals were provided supplemental snacks upon completion of each of the three parts of experimentation. This treat was either Cheeto cheese puffs or Pops sugar puff cereal. There were no contaminants suspected in either the diet or purified water that would be expected to have an effect upon the outcome of the study.

Procedures

Surgical Procedure

Surgical procedures were carried out based on the University of Kentucky DLAR standards of aseptic anesthetized animal surgery. Pre-surgical procedures were as follow: Isoflurane (Attane Isofulurane, USP liquid for inhalation) was replenished in the vaporizer and a heated water pad (Gaymar Industries, Inc, TP3E), connected to a water bath (Gaymar Industries, Inc, T/Pump, TP500), was set to 40 degrees celsius to maintain an animal body temperature of 37 degrees celsius. Animals were sedated in an induction chamber at 3.0-3.5% Isoflurane. Animals were then transferred to a stereotaxic frame (Koph Instruments) and secured into place with a palate clip and ear bars. Both the induction chamber and stereotaxic frame received vaporized Isoflurane from a Patterson Veterinary Vaporizer. The palate clip of the stereotaxic frame was set at -2.3 cm and ear bars entered the ear canal and were set at an average of -7.0 to -8.0 cm on either side to secure the head in a flat plane. Anesthetic was reduced to 2.0-2.5% for the remainder of the surgery. Animals were administered Rymadyl (5mg/mL) at 5mg/kg to mitigate pain from surgery. The animals' eyes were lubricated with lubricant eye ointment (Lubrifresh P.M (sterile) to prevent dry eyes or debris from entering their eyes. Animal heads were shaved near the intended site of incision from between the eyes to past the approximate

location of lambda. Betadine was then applied locally to the shaved area and two sterile alcohol prep pad wipes (Fisherbrand medium) followed to ensure a sterile site of incision.

An inch long incision was made in between the eyes using a 10 blade scalpel (Feather Surgical Blade and Handle stainless steel) that was extended approximately an inch caudally. Fascia was removed from the top of the skull and stainless-steel clamps were used to secure the fascia away from the surgical field. Cautery was used as needed to limit bleeding. Additionally, 0.9% saline solution and gauze pads were used to clear the surgical field of blood and debris as needed throughout the procedure. Bregma was identified and marked using a permanent marker (Sharpie), helping divide the surgical field into four identifiable quadrants. Three burr holes were made using a Dremel 107 bit (2.4mm) on a Froedom MH-170 surgical drill. These three holes, intended for screws, were placed into all of the quadrants except for the right rostral quadrant, which was reserved for S2 electrode implantation. An additional burr hole was made in the quadrant diagonal from the electrode quadrant. This hole was utilized later for placement of the reference electrode. A diagram of the schematic of the burr holes as seen on a dorsal view of the rat skull can be found in **FIGURE 1**. Screws were removed from their storage in isopropyl alcohol, rinsed with 0.9% saline solution and then screwed into the three burr holes. A rat's skull thickness can be anywhere from 0.5-1.0 mm (Paxino & Charles, 1998) and the screw threads were 2.0 mm. Once threaded, the screws were screwed in about 1mm to leave approximately 1.0 mm exposed above the skull.

The burr hole position for the electrode was approximated from bregma. The two subcortical areas of interest were measured as noted in **TABLE 3.2** found in the supplemental

images. All measurements were based on the atlas (Paxino & Charles, 1998) and were measured from the electrode tip, attached to the stereotaxic frame, from the center of bregma. Abbreviations for electrode implantation coordinates are Anterior-Posterior (AP), Medial-Lateral (ML), Dorsoventral (DV). Coordinates were for nucleus acuumbens were AP: -1.0, ML: -2.2, DV: +7.8 and AP: -3.2, ML -0.8 and DV: +5.5 for the frontal cortex. Forceps were used to ensure that the burr hole was smooth and perpendicular at all points, so the electrode would not touch any portion of the skull that was not clearly visible from the dorsal surface of the skull. The electrode was placed on the stereotaxic frame arm and the tip of the electrode was measured to a subcortical region from bregma using AP and ML measurements. Adjustments to the burr hole were made on an as-needed basis. This includes removing the electrode from the surgical field, via moving the stereotaxic frame arm, to drill further to enlarge the burr hole.

Once the electrode was aligned and deemed ready to be implanted, the Ag/AgCl reference electrode was placed into the reference burr hole. The electrode was implanted under the skull so that it sat parallel to the skull to minimize localized neuronal damage from the electrode implantation. The reference wire was then wrapped around the two posterior screws to secure it in place. The electrode was then implanted into the cortical area of interest. Electrode placements were confirmed post-mortem through cryostat brain sectioning (Gerhardt et al. 2018). Once the electrode was placed at the proper DV location, superglue and activator (Kwik-Fix project glue, Kwik-Fix activator) was applied to the electrode tip to secure the electrode into place. From this point, additional glue and activator was used to build a mound around the S2 apparatus. Clips were removed from

the surrounding fascia and the skin surrounding the surgical field was adhered to the S2 system.

The animal was taken off anesthesia, removed from the stereotaxic frame and returned to its housing unit that was placed on a heating pad. The heating pad helped maintain the animal's body temperature while regaining consciousness. Animals were monitored for three days post surgery. Daily weights were taken. Rymadyl was administered intramuscular daily in doses of 5 mg/kg. After this recovery period, animals were returned to the DLAR animal facility for housing for the next three weeks. Animals were run through the first study seven days after the surgical implantation date.

Experimental Procedure

Seven days after implantation of the MEA pedestals, rats were connected to a FAST Mark IV electrochemical recording system, which is controlled by a Labview/ Matlab software interface for real-time measures. Two animals were run simultaneously and always through the same computer and induction chamber throughout the course of the full experiment. Experiments were conducted no sooner than seven days following surgery and no sooner than five days following the previous experiment. This ensured sufficient amount of time for the animal to eliminate any test agents from their body (Gerhardt, Greg A, et al. 2018.). Experimentation took, on average, five hours. This time includes retrieving animals from the animal storage facility, induction and both rounds of test article administration. Experimentation had two sections. The first sections recordings took place at +0.6 V vs. Ag/AgCl. A baseline measure was recorded for 30 minutes before the nasal administration of test articles. Recordings continued for an

additional 1.5 hour. The recording were then reset to +0.2 V vs. Ag/AgCl and baseline was recorded for another 30 minutes. The designated test article was delivered by nasal delivery under sedation to determine possible noise and/or interference to the NO• signals. Recordings were continued for an additional 1.5 hours.

Prior to experimentation, animals were first induced in an induction chamber at 3.0-3.5% Isoflurane (Attane Isoflurane, USP liquid for inhalation). Once anesthetized, animals were weighed and attached to the head-stage of the Fast Analytical Sensing Technology (FAST) computer-controlled potentiostat system (FAST; Quanteon, Lexington, KY). The animals were positioned in a modified prone position with their heads angled upward towards the corner of the induction chamber to allow for easy nasal administration of the test articles. A depiction of this positioning is seen in **FIGURE 3.2**.

Once properly positioned and deemed sufficiently sedated, Isoflurane levels were reduced to 2.0% for the remainder of the first 30 minute baseline recordings. Test articles were retrieved from storage at 5 degrees celsius. Test and control articles were all made by the study director within 48 hours of experimentation and blinded to the experimenter through designations article A, B and C (Gerhardt et al. 2018). After the 30 minutes of recording a baseline signal, the test or control articles were administered by micropipette tips (Rainin micropipette). 125 µl of test agent was administered over a 5 to 6 minute period. 12.5 µl was administered per nostril with one minute wait periods in between the end of each article administration. This means that 25 µl was administered five times over an average of six minutes.

After nasal administration, recordings were continued for another 90 minutes under light sedation of 1.5-1.75% Isoflurane. Upon completion of the +0.6 V vs. Ag/AgCl recording, animals were maintained under sedation and run through the same experimental procedures at +0.2 V vs. Ag/AgCl, which was repeated over the following two hours. This recording was utilized to administer the designated test or control article again to determine possible noise and/or interference to the NO• signals recording for the final 90 minutes of the two hour total recording time. At the end of experimentation, animals were removed from anesthesia and returned to their home cages. The cages were placed on a heating pad to help maintain a normal body temperature until regaining consciousness. Animals were then returned to the University of Kentucky DLAR facility for a five day (minimum) anesthesia washout period. The remaining 2 of the 3 articles were administered over the course of the next two weeks, one per week. Thus, animals received 3 treatments over the 15-21 day period (Gerhardt et al. 2018).

Administration of test articles resulted in a variety of observable behaviors including change in respiration rate and depth. Often, following the second round of nasal administration, noticeable difficulty in breathing was observed. This was considered a potentially severe adverse outcome. Adverse outcomes are further documented in the corresponding subsection. Additionally, eye blink and reflexive head movements were observed during nasal administration in most animals. This was considered a consequential outcome from TA delivery and not an adverse outcome. Animals that displayed significant head jerk activity as a reflexive response to nasal administration of the test article were not repositioned to the modified prone position until at least 10 minutes following that round of nasal administration. This precaution was taken to ensure minimal interference with the FAST recording system during the minutes following TA administration.

Euthanization

At the completion of the testing of the 3 treatment recording days, rats were euthanized by Isoflurane sedation utilizing sustained level Isoflurane (4-5%) for up to five minutes until normal breathing was notably disrupted. Animals were subsequently decapitated, placed in a labeled bag and stored in a -18 degree freezer. Brains were removed later and sliced using a rat brain mold to confirm the location of the MEAs (Gerhardt et al. 2018).

Adverse Outcomes

Throughout the course of this experiment four animals did not finish experimentation and, consequently, new animals had to go through the acclimation period, surgery, recovery time and then run through the entire three part experiment. This group of animals includes three animals from the nucleus accumbens group and one animal from the frontal cortex arm of the study. The adverse outcomes included the loss of the animal's head cap, generally caused by the animal's own self mutilation by bumping its head, and death during experimentation. A more detailed list of fatal events are found in **TABLE 3.3.** The adverse event of head-caps falling off was determined to be caused by expired project glue (Kwik-Fix instant bond as well as adhesive). Following replacement of project glue with non-expired product, the issues of lost head-caps seen in animals #1 and #2 was not seen in any subsequent animals. The second fatal issue seen in Animals #5 and #9, death during experimentation, was determined to be due to poor circulation and aspiration of the test article during experimentation. After implementation of a heating pad for animal #8 (experiment 3) and animals #5 and #10, this issue of death due to insufficient respiration was not observed again. Animals that displayed severe respiratory disturbance following the second round of test article administration were moved to a full prone position to ease their breathing. This movement was made no sooner than 10 minutes following the end of the TA administration.

Non-fatal adverse outcomes were also observed throughout the course of experimentation. Mild respiratory distress was the most prevalent and most concerning adverse event. Changes in breathing were closely monitored during and following nasal administration of the test article. Generally, significant changes in respiratory rate and depth were observed

following the second round of nasal administration of the test article during the 0.6 V vs Ag/AgCl recording period. Other non-fatal adverse outcomes included, but were not limited to difficulty regaining consciousness post experimentation. This was defined as any time greater than 20 minutes after being removed from anesthesia. This event was observed in <5 animals.

Record Retention

Modifications in the study design were only made with verbal or written consent of the Study Director. Verbal authorization must be documented in the raw data and followed by a written protocol amendment within 10 business days. All amendments or deviations to the approved study protocol were documented, signed by the Study Director, dated, and maintained with the study protocol . All amendments to the approved study protocol were also approved by the Sponsor. After the final report is approved by the Study Director, all raw data and specimens relating to this study will be archived for up to 1 year. The test facility archives staff will contact the Sponsor after 1 year following report finalization to determine disposition of the archived materials (except for the raw data on durable media, study correspondence, and the copy of the final report). Portions of the study conducted by the sponsor or sponsor's designee will be archived in the storage facilities of the sponsor or sponsor's designee (Gerhardt et al. 2018).

Data Analysis

All data sets were analyzed by our Matlab based analysis system that involves FFT filtering, boxcar averages and averaging of data from the 4 sites of the MEAs prior to averaging of responses from the different animals. The low voltage measures were used to identify any interferences. Our detection limits *in vitro* are estimated to be in the 10-20 nanomolar range (Santos et al. 2011). *In vivo* results can vary due to physiological changes that may occur at the higher doses of test article administration. The studies were based in groups of 5 due to power analysis requirements. Power calculations using an α=0.05, β=0.10, and a detectable difference of 30-40% from baseline for the measures predict the necessary sample size of n=5 for the proposed studies. All data were analyzed using an Analysis of Variance (ANOVA) followed by appropriate post-hoc comparisons. Final data analyses is focused on the effects of the 3 treatments on maximum extracellular NO• ([NO]max) and kinetic data of the signals involving T_{rise}, $T_{1/2}$, T_{100}

(all in minutes). Note: these are discovery studies with no guarantee that the doses and route of administration of the NO• test article would produce detectable levels of NO• (Gerhardt et al. 2018).

	Treatment Day		
Animal	1	2	3
1	A	B	C
2	B	C	A
3	A	C	B
4	B	C	A
5	A	B	C

TABLE 3.1: RANDOMIZATION OF TREATMENT ORDER

This table depicts the randomization of treatment groups. The randomization order was followed for both groups (the two brain regions). As noted in the corresponding section, test or control articles were all made by the study director within 48 hours of experimentation and blinded to the experimenter through designations of article A, B and C (Gerhardt et al. 2018). Test and control articles are described by composition and concentration in the section labeled test and control articles. The experimenter was blinded to which article corresponded to each compound. This ensured that the order of test article administration did not confound results.

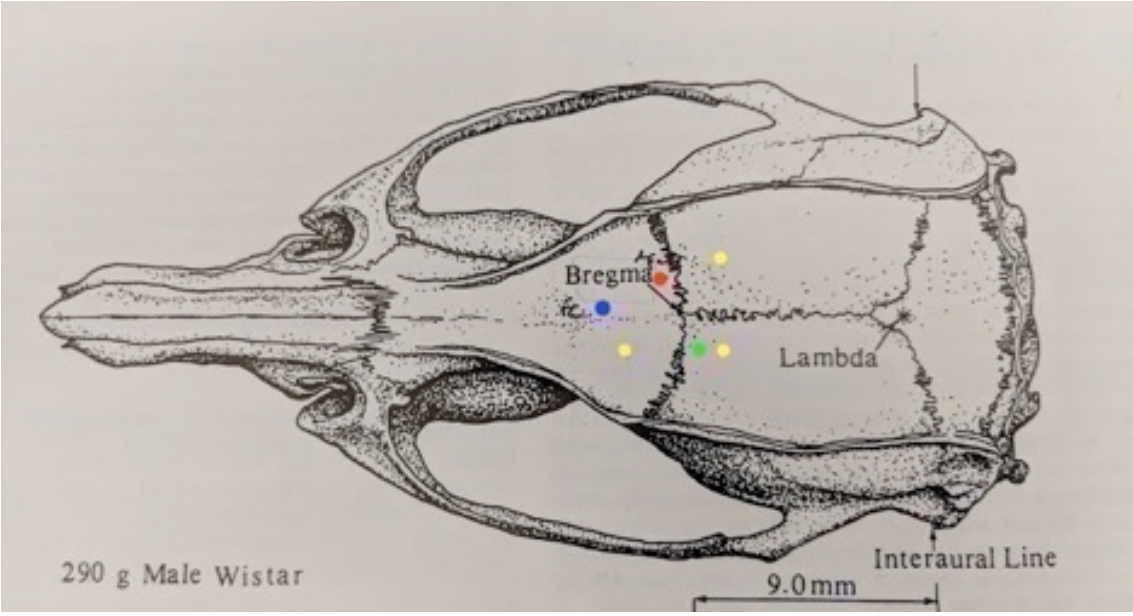

FIGURE 3.1: DORSAL SKULL VIEW

Depicted in the image above is the view of a rat skull as seen in *The Rat Brain: in Stereotaxic Coordinates* by George Paxino and Charles Watson. This image has been modified from the original text to include color coded dots that indicate the approximate location of burr holes that were made during the S2 implementation surgery. Yellow dots indicate the locations of screws and the green dot indicates the location of the Ag/AgCl reference electrode. The Ag/AgCl reference electrode burr hole is placed in the contralateral quadrant to minimize any noise or electrical interference from the S2 electrode and provide the best possible reference signal. The red dot indicates the location of the S2 electrode burr hole for the nucleus accumbens and the blue dot indicates the location of the S2 electrode implantation burr hole for measuring local nitric oxide levels in the rat frontal cortex. Note: all burr hole placements shown are approximate. During surgical implantation of the MEA, the two different regions for electrode placement were measured using the stereotaxic arm.

Nucleus Accumbens:	
AP	-1.0
ML	-2.2
DV	+7.8

Frontal Cortex:	
AP	-3.2
ML	-0.8
DV	+5.5

TABLE 3.2: SUBCORTICAL COORDINATES

Depicted above is a table of the A/P, M/L and D/V for the two subcortical areas of interest. All values are listed in millimeters. Subcortical locations were referenced based on (Paxino & Charles, 1998). These locations were measured using the stereotaxic frame (Koph Instruments) from bregma, as noted in (Paxino & Charles, 1998). The tip of the MEA was attached to the stereotaxic frame arm and placed directly above bregma and AP and ML measurements were made using this arm. Once the electrode was above the pre-drilled burr hole, the MEA was ensured to fit properly in the opening. If adjustments were necessary, the MEA on the arm was removed from the surgical field, necessary adjustments were made to the burr hole to ensure proper location of MEA placement. Then the MEA was again measured from bregma. DV was reset once the MEA tip came into contact with the dura. Once placement was correct, the process of applying the project glue and drying it with the Kwik-Fix activator was initiated.

Animal number	Number of experiments completed	Reason for not completing experimentation	Additional notes
Animal #1	1	lost head-cap	second animal #1 completed full experiment
Animal #2	1	lost head-cap	second animal #2 completed full experiment 11/8/18
Animal #5	1	death during experiment 2 due to respiratory distress	second animal #5 completed full experiment 12/17/18
Animal #9	1	death during experiment 2 due to respiratory distress	second animal #9 completed full experimentation 2/19

TABLE 3.3: ADVERSE OUTCOMES LEADING TO PREMATURE EXPERIMENTATION TERMINATION

Two adverse events resulted in premature death or euthanization. This included the loss of the animal's head-cap, the top of the MEA that held the attachment points to the four channel electrode as well as anchored the reference electrode wire. In one case, the head-cap popped off from excess pressure experienced from the attachment to the FAST system. In the other case, the animal, through self mutilation, caused the release of the head-cap from the skull by breaking the adhesive. Both animals were euthanized following the loss of the head-cap. Two animals died during experimentation from what was dubbed respiratory distress due to aspiration of the test article. The test articles administered to animals #5 and #9 were B and C, respectively. Both of these test articles contained nitroglycerin, although in different concentrations, but the chemical properties of nitroglycerin, as compared to miglyol, could potentially account for this outcome. However, this issue was resolved and not observed again after the implementation of heating pads during experimentation. This was utilized to help normalize circulation and body temperature during the experimentation of these anesthetized animals.

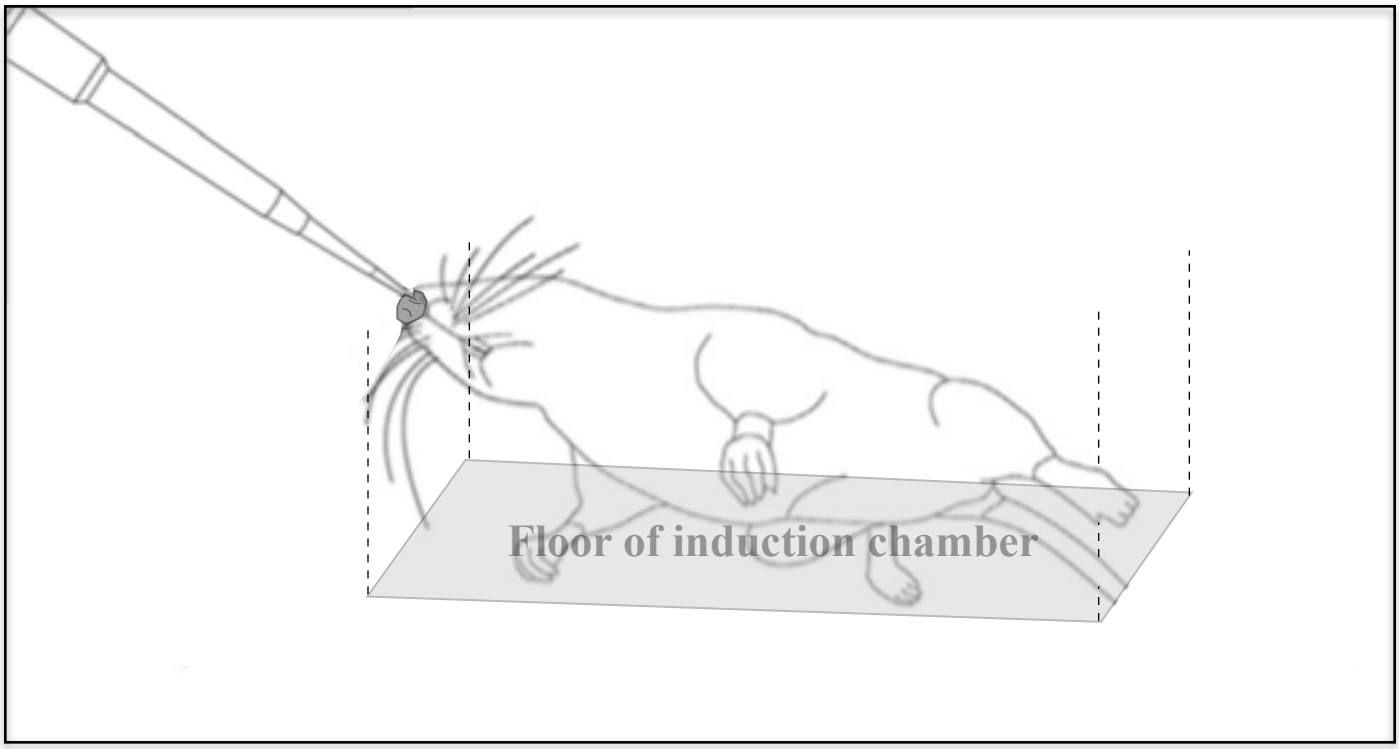

FIGURE 3.2: EXPERIMENTAL POSITIONING

The animal position during experimentation is depicted in the image (viewed from below the animal). Animals were positioned in this modified prone position to allow for easy nasal administration through the nostrils due to being exposed and easily accessible by micropipette tips. Shown in dashes is the induction chamber that the animals were placed in during experimentation. This rectangular box allowed the animals to rest on their belly while their heads were placed at a sharp upward angle to facilitate the nasal administration of test articles. During experimentation, the animal rested both of its cheeks on either side of the corner of the induction chamber.

Chapter Four: Results and Discussion

Results

In this study we used amperometric recording techniques coupled with a 4-channel low noise pre-amplifier system and new generation microelectrode arrays (MEAs) with high spatial (µm) and temporal (100 Hz) resolution to explore *in vivo* effects of an FDA-approved NO• donor (nitroglycerin) on extracellular levels of NO• in the frontal cortex and nucleus accumbens of lightly anesthetized Wistar rats following intranasal administration. FAST recording system was utilized to record the full four hour experiment. An example of a tracing produced from the experiment can be seen in **FIGURE 4.1**.

Frontal Cortex

The results of the frontal cortex, as seen in **FIGURE 4.2**, do not show any significant difference in measured extracellular NO• levels between the three treatment groups, myglol, 10 mg/kg nitroglycerin (NG) and 15 mg/kg nitroglycerin. The average value of the area under the curve (AUC) was ~1,000, ~1,000 and ~1,000 for myglol, NG10mg/kg and NG 15mg/kg, respectively. While the 95% does include 0 for all compounds except the 15mg/kg Nitroglycerin dose, meaning the nasal administration of the other two compounds could, theoretically, not cause a localized extracellular increase in NO• in the frontal cortex at all, it is likely with increased sample size (N) that there would be significant difference from 0 for all three compounds. However, there is no significant difference between the increased extracellular concentration of NO• following nasal administration of NG as compared to myglol.

Nucleus Accumbens

The results of the nucleus accumbens, as seen in **FIGURE 4.3**, do not show any significant difference in measured extracellular NO• levels between the three treatment groups, myglol,10 mg/kg nitroglycerin and 15 mg/kg nitroglycerin. The average value AUC was much higher than for the frontal cortex at ~4,000, ~5,000 and ~4,000 for myglol, NG10mg/kg and NG 15mg/kg, respectively. While the 95% does include 0, meaning the nasal administration of all three compounds could not cause a change in extracellular NO• in the nucleus accumbens, it is likely with increased sample size (N) that there would be significant difference from 0 for all

three compounds. While there is no significant difference between the increased extracellular concentration of NO• following nasal administration of NG as compared to myglol, it is interesting to note that the average AUC values of all three test articles are approximately five times higher than those measured in the frontal cortex.

Conclusions

This study was unable to conclude there was a significant difference in the level of extracellular nitric oxide measured in the rat frontal cortex and nucleus accumbens following the nasal administration of nitroglycerin, a widely accepted nitric oxide donor, when compared to the placebo of Miglyol. It does suggest that nasal administration of myglol may cause a significant increase in extracellular nitric oxide in the two subcortical areas of interest. This could be due to a physiological response to nasal administration. This theory suggest that, regardless of the compound, nasally administered substances cause a response in animals that causes increased extracellular NO• in the two subcortical areas. A way to test this theory is to add an additional control of saline, as myglol itself has to be ruled out from causing the observed effect.

There are many hypotheses as to why nitroglycerin did not significantly effect the extracellular concentration of NO•. Firstly, there is the chance that NG was not able to enter the CNS through the nasally administered drug route described in the section, "Intranasal drug administration". While the chemical properties of nitroglycerin suggests the drug should be able to cross the sustentacular cells via receptor mediated endocytosis and enter the brain, nitroglycerin may not easy utilize this so called transcellular pathway. Additionally, the drug may not be able to enter the brain via transversing tight junctions of sustentacular cells in the paracellular pathway. It was already demonstrated in previous research that, despite following all of Lipinksi's rules except for the number of H bond donors, nitroglycerin does not seem to effectively cross the blood brain barrier. See section, "Intraperitoneal Studies" for more information. A final possible reason as to why nitroglycerin is not able to cause increased extracellular NO• is that, despite entering the CNS properly via the aforementioned pathways, once nitroglycerin is oxidized, the NO• generated is rapidly inactivated by the brain's vasculature as described in the section "Decay and Removal".

Interestingly, average AUC measured in the nucleus accumbens was, on average, 5 times greater than the frontal cortex. One interpretation of these results includes the notion that there is a higher NOS concentration in the nucleus accumbens as compared to other cortical structures (Vincent and Kimura, 1992). A study conducted by Vincent and Kimura selectively stained the rat brain for NADPH-diaphorase. This enzyme provides a specific histochemical marker for the production of NO•. Their results showed that the striatum exhibited some of the heaviest staining. Additionally, in humans, the highest levels of nNOS were measured in the nucleus accumbens, along with other structures such as the cerebellar cortex and septal area (Bernstein et al., 2005). This notion that there is a high NOS concentration in the nucleus accumbens is supported by the results we reported in this study. However, further research needs to be conducted within this area to fully elucidate the basal concentration of NOS and NO• signaling throughout the brain.

Future Directions

Intraperitoneal Studies

A previous study looked into the effects of three nitric oxide donors on extracellular NO• concentrations in the frontal cortex and nucleus accumbens following intraperitoneal administration. While none of the NO• donors were found to have a significant effect, as seen in **TABLE 4.3** and **TABLE 4.4**, one drug, molsidomine, showed promise as causing significant changes in extracellular NO• in the two subcortical areas, particularly the frontal cortex. It is an important consideration that these studies were conducted in awake wistar rats, as compared to the light sedation used in the nitroglycerin study. It is additionally interesting to note the differences in the average AUC for the two studies. For the frontal cortex averages for the AUC were ~800 for molsidomine, ~300 for nitroglycerin, ~200 for saline and ~200 for myglol-saline. Similar averages were found in the nucleus accumbens with the exception of myglol-saline and molsidomine which both had an average AUC of ~1,000. It is interesting to note that, within the intraperitoneal study alone, there was no large difference found between the average AUC in the frontal cortex as compared to the nucleus accumbens. This is an important difference between this study and the reported intranasal study.

Molsidomine

Molsidomine is a nitric oxide donor with the chemical formula of $C_9H_{14}N_4O_4$ (Aronson & Meyler, 2016). This compound is FDA approved to treat angina pectoris, acute myocardial infarction, congestive heart failure and pulmonary hypertension in oral and injectable forms (Rosenkranz et al., 1996). The prodrug is metabolized to SIN-1, an active metabolite, and NO through hydrolysis and decarboxylation in the liver and has a half-life of 1 to 2 hours. The bioavailability through oral administration is 44-59%. This compound, as displayed in the section, "Intraperitoneal Studies" is a possible candidate for intranasal administration. While the IP studies did not yield a significant result for Molsidomine, an increase in the concentration of drug administered, number of animals run through the study and potential greater uptake of the compound through intranasal means (as compared to systemic administration) could yield significant results. Furthermore, Molsidomine follows all of Lipinski's rule of 5 with sufficiently low molecular weight, LogP, H bond donor atoms and H bond receptor atoms. This is interesting considering that nitroglycerin does not follow one of Lipinski's rules by having too many H bond donor atoms.

A large concerns with continuing intranasal research of NO• donor prodrugs include the rate at which the prodrug is converted to NO• in the brain parenchyma. It is quite plausible that the drug is converted to metabolites, SIN-1 in the case of molsidomine, and NO• prior to reaching the target cortical structures and therefore it can not cause a localized increase in extracellular NO• concentrations. Instead, the NO• is potentially rapidly inactivated by the brain's dense vasculature system as NO• has been suggested to rapidly diffuse through epithelial cells to enter the vasculature (Santos et al., 2011).

Intranasal Nitroglycerin

The results of this study support nitroglycerin, without co-administration with another compound, as a poor candidate to continue further intranasal drug development studies. The lack of a significant difference, as compared to myglol, suggests that there is insufficient nitric oxide donated from nitroglycerin reaching the target cortical structures. As stated previously, there are multiple way in which this lack of increased extracellular NO• could occur. Other issues that arise with any intranasal drug is the lack of specificity. Distribution of nasally administered compounds

can vary depending on the chemical properties of the drug. While a large proportion of the compound can remain in the olfactory region (olfactory nerve and bulb), a lack of permeability into deep cortical structures is not likely the cause of not statistically significant results since permeability into the striatum and substantia nigra has been observed for nasally administered DNSP-11 (Stenslik et al., 2015). A final consideration is the understood role of NO• donors in causing headaches and migraines. If an intranasal NO• donor was to enter stage 1 clinical, it is likely there would be mild to moderate side effects of headaches. This could interfere with drug dosage and tolerability.

In the future, alternative NO• donor molecules, such as molsidomine, which have shown promise for significantly altering extracellular NO• in the nucleus accumbens and especially in the frontal cortex, should be considered for further investigation. I propose an identical study be run with an additional test agent of saline, to control for the effects of myglol, as well as behavioral and cognitive testing before and after drug administration to scan for behavioral changes in the animals that could translate to side effect profiles and tolerability in humans.

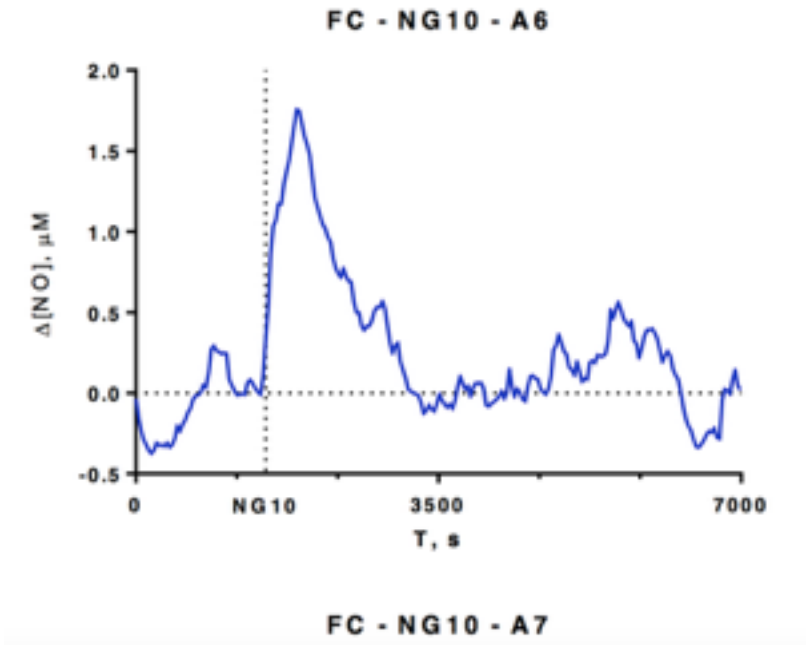

TABLE 4.1: EXPERIMENTAL TRACING, ANIMAL 6 NG-10

The above tracing shows the data yielded from an experiment. The graph depicts time on the Y axis and the change in the concentration of NO• in µM on the Y axis. This particular tracing is from animal 6 with the test article nitroglycerin 10mg/kg dosage. Where the two dashed lines intersect is the point at which nasal administration began. The tracing continues throughout the end of the experiment. While this example shows remarkable changes in the µM concentration of NO•, in total over the 5 animals, no statistically =significant result was seen.

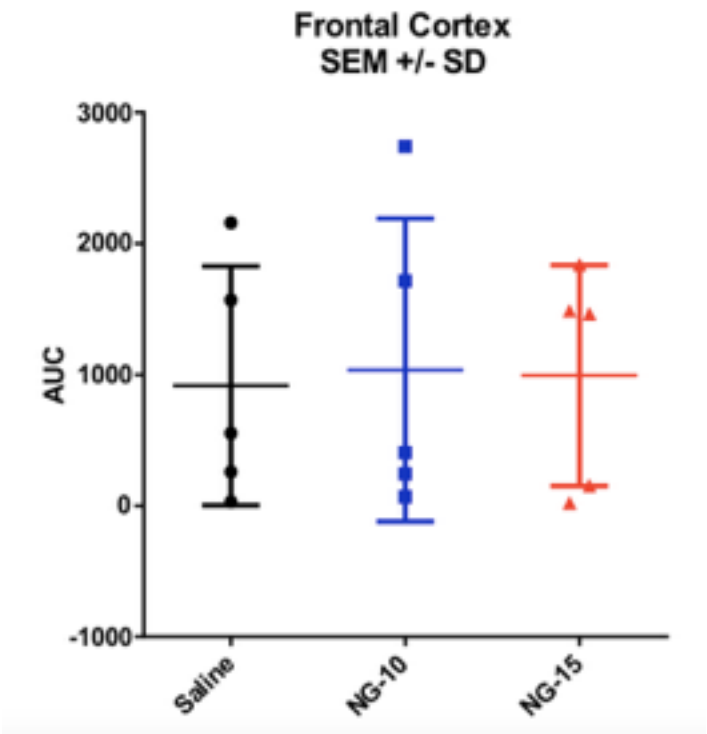

TABLE 4.2: AUC OF TEST ARTICLES IN THE FRONTAL CORTEX

Depicted above is the recorded AUC in the frontal cortex for the three treatments in this study: myglol, nitroglycerin 10mg/kg (NG-10) and nitroglycerin 15mg/kg (NG-15). the 15mg/kg dosage of nitroglycerin was the only compound to not contain the value “0” in its 95% CI.

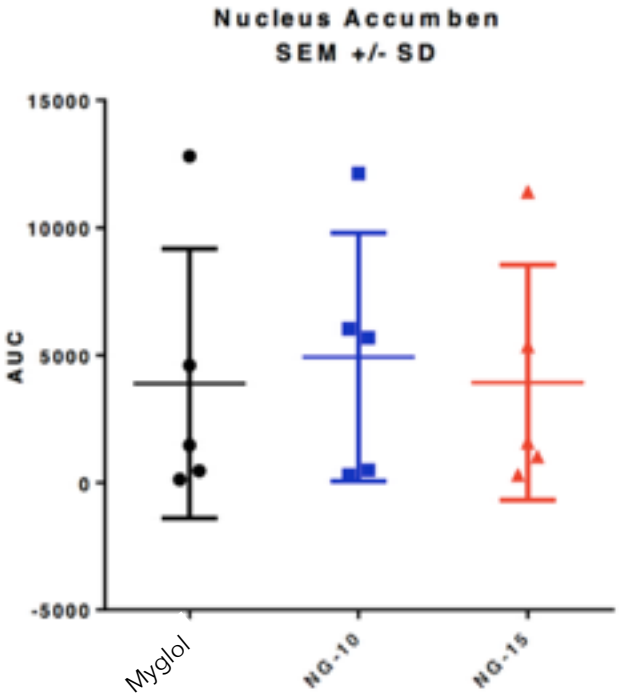

TABLE 4.3: AUC OF TEST ARTICLES IN THE NUCLEUS ACCUMBENS

Depicted above is the recorded AUC in the nucleus accumbens for the three treatments in this study: myglol, nitroglycerin 10mg/kg (NG-10) and nitroglycerin 15mg/kg (NG-15). None of the compounds elicited significant changes in extracellular nitric oxide concentrations, as seen by the 95% CI that contain the AUC value "0".

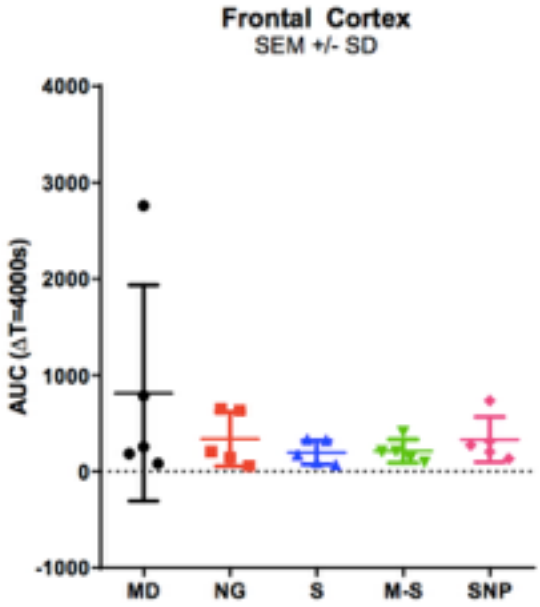

TABLE 4.4: EXTRACELLULAR NO• LEVELS IN THE FRONTAL CORTEX FOLLOWING INTRAPERITONEAL ADMINISTRATION OF NO• DONORS

Depicted above is the recorded AUC in the frontal cortex for the five treatments in this study: molsidomine (MD), nitroglycerin (NG), saline (S), myglol-saline (M-S) and SNP, a known NO• donor. None of the compounds elicited significant changes in extracellular nitric oxide concentrations, as seen by the 95% CI that contain the AUC value "0". However, it is interesting to note how much larger the average AUC for molsidomine was as compared to the other NO• donors, nitroglycerin and SNP.

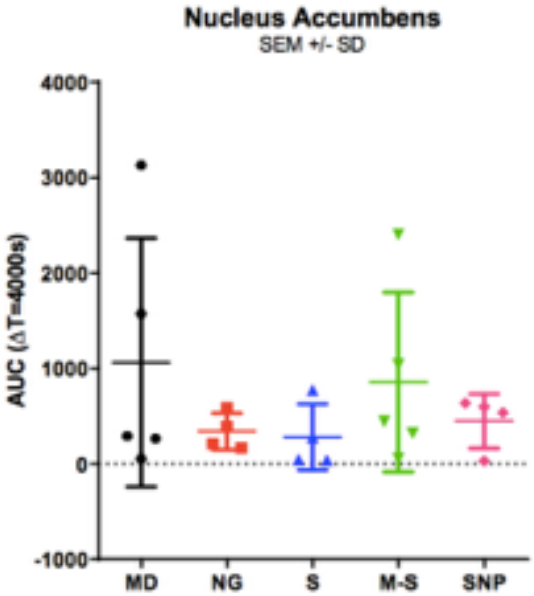

TABLE 4.5: EXTRACELLULAR NO• LEVELS IN THE NUCLEUS ACCUMBENS FOLLOWING INTRAPERITONEAL ADMINISTRATION OF NO• DONORS

Depicted above is the recorded AUC in the frontal cortex for the five treatments in this study: molsidomine (MD), nitroglycerin (NG), saline (S), myglol-saline (M-S) and SNP, a known NO• donor. None of the compounds elicited significant changes in extracellular nitric oxide concentrations, as seen by the 95% CI that contain the AUC value "0". It is interesting to note that molsidomine and myglol-saline had higher average AUCs as compared to the other three test articles.

References

Bernstein, Hans-Gert, et al. “The Many Faces of Nitric Oxide in Schizophrenia. A Review.” Schizophrenia Research, vol. 78, no. 1, 2005, pp. 69–86., doi:10.1016/j.schres.2005.05.019.

Choudhari, Sheetal Korde, et al. “Nitric Oxide and Cancer: a Review.” World Journal of Surgical Oncology, vol. 11, no. 1, 2013, doi:10.1186/1477-7819-11-118.

Ekhtiari, Hamed, and Martin P. Paulus. Neuroscience for Addiction Medicine: from Prevention to Rehabilitation. Elsevier, 2016.

Floresco, Stan B. “The Nucleus Accumbens: An Interface Between Cognition, Emotion, and Action.” Annual Review of Psychology, vol. 66, no. 1, 2015, pp. 25–52., doi:10.1146/annurev-psych-010213-115159.

Friedemann, Marilyn N., et al. “o-Phenylenediamine-Modified Carbon Fiber Electrodes for the Detection of Nitric Oxide.” Analytical Chemistry, vol. 68, no. 15, 1996, pp. 2621–2628., doi: 10.1021/ac960093w.

Garthwaite, J. “Nitric Oxide Signaling in the Central Nervous System.” Annual Review of Physiology, vol. 57, no. 1, 1995, pp. 683–706., doi:10.1146/annurev.physiol.57.1.683.

Garthwaite, John. “NO as a Multimodal Transmitter in the Brain: Discovery and Current Status.” British Journal of Pharmacology, vol. 176, no. 2, 2018, pp. 197–211., doi:10.1111/bph.14532.

Gerhardt, Greg A, et al. Rapid NO Measures in Rat Nucleus Accumbens and Frontal Cortex Following Nasal Administration. BDD Berolina Drug Development GmbH, 2018.

Gow, A. J., et al. “The Oxyhemoglobin Reaction of Nitric Oxide.” Proceedings of the National Academy of Sciences, vol. 96, no. 16, 1999, pp. 9027–9032., doi:10.1073/pnas.96.16.9027.

Hardingham, Neil, et al. “The Role of Nitric Oxide in Pre-Synaptic Plasticity and Homeostasis.” Frontiers in Cellular Neuroscience, vol. 7, 2013, doi:10.3389/fncel.2013.00190.

Hascup, K. N., et al. “Second-by-Second Measures of L-Glutamate in the Prefrontal Cortex and Striatum of Freely Moving Mice.” Journal of Pharmacology and Experimental Therapeutics, vol. 324, no. 2, 2007, pp. 725–731., doi:10.1124/jpet.107.131698.

Hascup, Kevin, et al. “Second-by-Second Measures of L-Glutamate and Other Neurotransmitters Using Enzyme-Based Microelectrode Arrays.” Frontiers in Neuroengineering Series Electrochemical Methods for Neuroscience, 2006, pp. 407–450., doi: 10.1201/9781420005868.ch19.

Herman, Barbara H, et al. “The Effects of NMDA Receptor Antagonists and Nitric Oxide Synthase Inhibitors on Opioid Tolerance and Withdrawal.” Neuropsychopharmacology, vol. 13, no. 4, 1995, pp. 269–293., doi:10.1038/sj.npp.1380298.

Illum, Lisbeth. “Nasal Drug Delivery—Possibilities, Problems and Solutions.” Journal of Controlled Release, vol. 87, no. 1-3, 2003, pp. 187–198., doi:10.1016/s0168-3659(02)00363-2.

Illum, Lisbeth. “Transport of Drugs from the Nasal Cavity to the Central Nervous System.” European Journal of Pharmaceutical Sciences, vol. 11, no. 1, 2000, pp. 1–18., doi:10.1016/s0928-0987(00)00087-7.

Kolb, B. “Functions of the Frontal Cortex of the Rat: A Comparative Review.” Brain Research Reviews, vol. 8, no. 1, 1984, pp. 65–98., doi:10.1016/0165-0173(84)90018-3.

“Molsidomine.” Meyler's Side Effects of Drugs: the International Encyclopedia of Adverse Drug Reactions and Interactions, by J. K. Aronson and L. Meyler, Elsevier, 2016, pp. 1085–1085.

Paxino, George, and Charles Watson. The Rat Brain: in Sterotaxic Coordinates. Academic Press, 1998.

Prast, H., et al. “Nitric Oxide-Induced Release of Acetylcholine in the Nucleus Accumbens: Role of Cyclic GMP, Glutamate, and GABA.” Journal of Neurochemistry, vol. 71, no. 1, 2002, pp. 266–273., doi:10.1046/j.1471-4159.1998.71010266.x.

Privett, Benjamin J., et al. “ChemInform Abstract: Electrochemical Nitric Oxide Sensors for Physiological Measurements.” ChemInform, vol. 41, no. 42, 2010, doi:10.1002/chin.201042277.

Reif, A, et al. “A Neuronal Nitric Oxide Synthase (NOS-I) Haplotype Associated with Schizophrenia Modifies Prefrontal Cortex Function.” Molecular Psychiatry, vol. 11, no. 3, 2006, pp. 286–300., doi:10.1038/sj.mp.4001779.

Ritz, M C, and M J Kuhar. “Psychostimulant Drugs and a Dopamine Hypothesis Regarding Addiction: Update on Recent Research.” Biochemical Society Symposium , vol. 54, 1993, pp. 51–64.

Rosenkranz, Bernd, et al. “Clinical Pharmacokinetics of Molsidomine.” Clinical Pharmacokinetics, vol. 30, no. 5, 1996, pp. 372–384., doi:10.2165/00003088-199630050-00004.

Rutherford, Erin C., et al. “Chronic Second-by-Second Measures of l-Glutamate in the Central Nervous System of Freely Moving Rats.” Journal of Neurochemistry, vol. 102, no. 3, 2007, pp. 712–722., doi:10.1111/j.1471-4159.2007.04596.x.

Santos, Ricardo M., et al. “Brain Nitric Oxide Inactivation Is Governed by the Vasculature.” Antioxidants & Redox Signaling, vol. 14, no. 6, 2011, pp. 1011–1021., doi:10.1089/ars.2010.3297.

Santos, Ricardo M., et al. “Evidence for a Pathway That Facilitates Nitric Oxide Diffusion in the Brain.” Neurochemistry International, vol. 59, no. 1, 2011, pp. 90–96., doi:10.1016/j.neuint.2011.05.016.

Smith, Bret. “Cellular Neurophysiology LTP.” ANA636. Aug. 2018, Lexington, Kentucky.

Stenslik, Mallory J., et al. “Methodology and Effects of Repeated Intranasal Delivery of DNSP-11 in a Rat Model of Parkinson's Disease.” Journal of Neuroscience Methods, vol. 251, 2015, pp. 120–129., doi:10.1016/j.jneumeth.2015.05.006.

Tassorelli, C, et al. “The Effects on the Central Nervous System of Nitroglycerin—Putative Mechanisms and Mediators.” Progress in Neurobiology, vol. 57, no. 6, 1999, pp. 607–624., doi:10.1016/s0301-0082(98)00071-9.

Teffer, Kate. “Human Prefrontal Cortex: Evolution, Development, and Pathology.” Progress in Brain Research, vol. 195, 2012, pp. 191–218., doi:10.1107/s0108768107031758/bs5044sup1.cif.

Vincent, S.r., and H. Kimura. “Histochemical Mapping of Nitric Oxide Synthase in the Rat Brain.” Neuroscience, vol. 46, no. 4, 1992, pp. 755–784., doi:10.1016/0306-4522(92)90184-4.

VITA

Name: Victoria A. Scott

Birthplace: Frankfort, Kentucky

Education

2018-2019 M.S., Medical Sciences, University of Kentucky

2015-2017 B.S., Neuroscience, Vanderbilt University

2014-2015 Biology, George Washington University

Employment History

2011-2018 Medical Records Clerk and Medical Assistant, Scott and Jonah, PSC

2015-2017 Research Assistant, Department of Biological Sciences, Vanderbilt University, Laboratory of Patrick Abbot, Ph.D.

2016-2018 Research Assistant, Department of Neuroscience, Vanderbilt University, Laboratory of Frank Tong, Ph.D.

2014-2015 Greenhouse Assistant, Department of Biological Sciences, George Washington University, Supervised by Robert Perry

Scholastic and Professional Honors

2017 Dean's List, Vanderbilt University, Nashville, Tennessee

2014 Merit Scholarship, George Washington University, Washington, District of Columbia

Professional Publications

May 25, 2017 Poster Presentation, APS Annual Convention, Boston, Massachusetts titled "The Vanderbilt Face Memory Test: A Novel and Sensitive Method of Facial Recognition"